Green Industrial Policy in a Globalized Economy [*†]

Sungwan Hong
University of Pittsburgh

October, 2025

Abstract

How does green industrial policy work in a globalized economy where renewable-energy equipment (solar panels, wind turbines) is traded? I build a dynamic trade model with traded capital equipment and learning-by-doing and apply it to the U.S. Inflation Reduction Act (IRA), which combines renewable-energy production and equipment-manufacturing subsidies. The instruments differ in terms-of-trade effects and the locus of learning: an energy subsidy increases imported equipment and raises global welfare more than U.S. welfare; an equipment subsidy concentrates learning at home and does the reverse. The IRA cuts global CO_2 by 0.63% and raises U.S. and global welfare by 0.05% and 0.03%, respectively.

JEL codes: F13, F18, O25, Q4, Q54, Q56

Keywords: Green Industrial Policy, Inflation Reduction Act, Energy Transition, Renewable Energy Equipment Trade

[*]I am grateful to Fernando Parro, Jingting Fan, and Stephen Yeaple for their guidance. I appreciate suggestions and comments from Kai-Jie Wu, Seula Kim, Yan Bai, Xiang Ding, Sharat Ganapati, Costas Arkolakis, Haruka Takayama, David Hemous, Konstantin Kucheryavyy, Johannes Boehm, Eugenie Dugoua, David Atkin, George Alessandria, Allan Hsiao, Jevan Cherniwchan, and seminar and conference participants at Penn State, University of Pittsburgh, Aarhus University, World Bank, Sogang University, Keio University, Kyoto University, Hitotsubashi University, University of Tokyo, AERE Summer Conference, RMET, and Midwest International Trade Conference. All errors are mine.

[†]Disclosure: This research received no external funding. I have no financial relationships or other conflicts of interest to disclose. The views expressed are my own. Correspondence by email: sungwan.hong@pitt.edu

1 Introduction

Global emissions remain off track for long-run climate targets, and many governments have turned to *green industrial policy* to accelerate the energy transition. A prominent example is the U.S. Inflation Reduction Act (IRA), which couples demand-side subsidies for renewable-energy production with supply-side support for domestic manufacturing of renewable-energy equipment—henceforth, the *energy subsidy* and the *equipment subsidy*.[1] Although the IRA is national in scope, equipment production is embedded in international supply chains.

Most quantitative evaluations adopt a closed-economy lens, abstracting from trade in clean-energy equipment and from how domestic subsidies transmit across borders (Arkolakis and Walsh, 2023; Bistline et al., 2023; Casey et al., 2023; Donald, 2024; Gentile, 2024). Whereas renewable energy itself is rarely traded across borders, its equipment (e.g., solar panels and wind turbines) is heavily traded, with production concentrated in a small set of countries. For example, U.S. and EU meet about 83% and 95% of domestic solar-equipment demand with imports, respectively, while China produces roughly 80% of global supply. Ignoring this margin can lead to different implications about subsidy incidence and the direction of cross-border spillovers.

I examine the domestic and global impacts of the U.S. Inflation Reduction Act (IRA) through an open-economy lens, focusing on its two instruments—an energy subsidy and an equipment subsidy—both separately and in combination. I build a multi-country dynamic general equilibrium model with international input–output linkages à la Caliendo and Parro (2015) in which (i) solar and wind equipment are traded capital goods that accumulate over time; (ii) electricity is produced with installed equipment (renewables) and fossil inputs in a nested CES energy block; (iii) equipment productivities evolve endogenously via external learning-by-doing (LBD); and (iv) CO_2 emissions generate a global externality. Subsidies enter as ad valorem output support to renewable energy or to equipment.

Two features organize the open-economy incidence of the IRA. First, because the U.S. relies on imported equipment and electricity is effectively nontraded, an equipment subsidy loads onto traded margins, and an energy subsidy loads onto nontraded domestic generation costs. Second, because of LBD, today's geography of production feeds back into future costs at home and abroad.

These features imply distinct mechanisms for each instrument. An energy subsidy raises domestic demand for renewable equipment that is largely met by imports from incumbent producers, boosting their scale and productivity via LBD; the abatement it delivers is concentrated in the subsidizing country, while lower world fossil prices and higher equipment prices can induce carbon leakage abroad. An equipment subsidy directly lowers domestic unit costs, expands home output, and displaces foreign production; by increasing global equipment supply, it reduces world equipment

[1] Examples of green industrial policies include the EU's Green Deal Industrial Plan, India's Production-Linked Incentive (PLI) scheme for solar modules, and Japan's Green Transformation (GX) plan.

prices, enabling other countries to accelerate deployment and cut emissions more broadly.

These channels map into heterogeneous cross-country incidence: upstream equipment exporters tend to gain from foreign energy subsidies (via higher demand), whereas net importers benefit—and net exporters lose—under foreign equipment subsidies (via cheaper imported equipment and reallocated learning). Because the climate benefit is common but the non-carbon (real-income) component can move in opposite directions, total welfare differs by country. Closed-economy analyses blur these margins and can misstate both welfare and emissions consequences; whether the IRA, or its components, are net beneficial for a given country or for the world is ultimately a quantitative question.

The model is disciplined by country–sector data from input–output tables and trade flows, and augmented with geospatial measures of renewable potential (solar irradiance and wind resource) that anchor cross-country absolute advantage and the slope of within-country decreasing returns in renewable energy generation. Most central to the model's dynamic mechanism are the LBD elasticities for solar and wind equipment, which I estimate by inverting trade shares to recover country-year productivities and regressing them on discounted cumulative output. To ensure a realistic energy mix, I also estimate the substitution elasticity between solar and wind using panel data on relative outputs and prices. Together, these primitives are crucial in governing the speed of the transition in each country: abundant potential combined with higher substitution and stronger learning implies faster deployment and cost reductions, whereas scarce potential, lower substitution, and weaker learning slow the transition.

With the model disciplined by data, I quantify the IRA's effects on emissions and welfare and decompose welfare into economic (real-income) and climate (carbon) components.[2] I show that outcomes are governed by the distinct transmission channels of the two instruments, revealing a measurable trade-off between preserving global specialization and building new comparative advantage in the U.S.

The energy subsidy primarily operates through the domestic renewable–fossil wedge in the energy block. Quantitatively, it reduces global CO_2 by 0.16% with abatement concentrated in the U.S. While the climate benefit is positive worldwide, the U.S. is a net importer of renewable equipment in the baseline, so part of the fiscal outlay passes through into higher revenues for incumbent foreign equipment producers. Consistent with this terms-of-trade mechanism, U.S. real income falls 0.06% and U.S. welfare falls 0.04%. At the same time, the rest of the world benefits from cheaper energy services induced by the U.S. demand surge, so global welfare rises 0.03%. In short, the energy subsidy preserves current specialization patterns, yielding a global welfare gain at the expense of the U.S.

The equipment subsidy acts through equipment trade and reallocation of production shares. It cuts global CO_2 by 0.27%—a larger emissions effect than the energy subsidy—and raises U.S. real

[2] Welfare equals discounted sum of real income plus a carbon benefit from lower CO_2.

income 0.06%, translating into a U.S. welfare gain of 0.08%. These gains arise because the policy pulls manufacturing onshore, lowers U.S. delivered equipment costs, and redirects learning-by-doing toward domestic producers. The flip side is weaker external learning and diminished gains from specialization for incumbent exporters. In the aggregate, the economic loss abroad offsets the U.S. gains, leaving global real income negative and global welfare approximately unchanged.

The full IRA combines these channels. The package lowers global CO_2 by 0.63% by 2100, with roughly one quarter of the abatement occurring outside the U.S. via price spillovers. Both U.S. and global welfare rise—by 0.05% and 0.03%, respectively—even as global real income effect is negative -0.04%. This pattern highlights the core trade-off: onshoring equipment production improves the U.S. terms of trade and domestic learning but weakens foreign learning and gains from global specialization; the net global welfare gain is therefore driven by the climate component.

Optimizing from the U.S. perspective tilts support toward an equipment subsidy rate of 40 percent (and 0 percent for energy). This mix amplifies the onshoring and learning channels, lowering global CO_2 by about 0.79% and raising U.S. welfare to 0.15% while leaving global welfare essentially flat. The gains for the U.S. come from cheaper domestic equipment, redirected learning, and improved terms of trade; the flat global welfare reflects the same specialization trade-off operating more strongly.

Accounting for equipment trade is crucial; abstracting from it changes the welfare incidence. In a counterfactual world without equipment trade, the IRA delivers a smaller global emissions reduction (0.42%), a smaller U.S. welfare gain (0.04%), and a larger global welfare gain (0.06%). A larger share of the welfare gains accrues outside the U.S. because the beggar-thy-neighbor channel is shut down when foreign producers cannot be displaced; conversely, the U.S. loses the ability to leverage export markets to accelerate learning-by-doing, muting domestic benefits and shrinking the overall emissions impact.

I then consider two departures from the baseline IRA. First, layering a sizable, U.S. tariff on imported solar equipment raises imported equipment prices, slowing the energy transition. The tariff slightly worsens CO_2 abatement and reduces welfare for both the U.S. and the world. Second, when major economic blocs (e.g., the EU and China) adopt IRA-like policies in parallel, global equipment costs fall and adoption spreads more broadly. In the multilateral case, U.S. equipment production does not expand; yet as a net importer, the U.S. benefits from foreign subsidies that raise global supply and lower world equipment prices, reducing domestic investment costs and speeding the transition.

Related Literature. This paper relates to three strands of literature.

First, this paper relates to the industrial-policy literature in open economies, from classical analyses (Baldwin, 1969; Bardhan, 1971; Ethier, 1982; Krugman, 1987) to recent quantitative trade evaluations (Goldberg et al., 2024; Lashkaripour and Lugovskyy, 2023; Ju et al., 2024; Bartelme et al., 2024; Choi and Levchenko, 2025). It adds to this literature by analyzing the global welfare im-

plications of unilateral green industrial policies in a dynamic open-economy framework that makes explicit two externalities—(i) a *global* carbon externality and (ii) a *local* learning-by-doing externality in renewable-equipment manufacturing—which together drive global carbon outcomes and heterogeneous global welfare implications.

Second, this paper contributes to the general-equilibrium analysis of clean-energy subsidy design—including IRA provisions—by contrasting energy-production subsidies with equipment-manufacturing support in a dynamic *open-economy* setting.[3,4] Related GE analyses are often developed in *closed-economy* environments (Donald, 2024; Gentile, 2024; Casey et al., 2023; Bistline et al., 2023). A notable exception is Arkolakis and Walsh (2023), who develop a dynamic spatial model with a detailed electricity grid and evaluate an energy-production subsidy under the IRA while abstracting from equipment trade. In contrast, I show that accounting for equipment trade reverses the U.S. welfare effect: the IRA's energy subsidy reduces U.S. welfare by worsening the terms of trade, whereas the IRA's equipment subsidy raises it; cross-country incidence varies with countries' net equipment-trade positions (net importers vs. net exporters). A separate line of work, Shin (2024), emphasizes factor-reallocation frictions in a global GE setting. I instead focus on dynamic equipment trade to quantify how energy and equipment subsidies differentially shape global welfare and carbon emissions in a unified framework.

Third, the paper builds on quantitative trade models with input–output linkages and multi-sector, multi-country structure, and on the environmental trade literature that emphasizes leakage, terms-of-trade, and coordination. The model adopts gravity-based discipline for trade elasticities and sectoral structure (Eaton and Kortum, 2002; Caliendo and Parro, 2015; Eaton et al., 2016), embeds an explicit energy nest, and features traded renewable equipment with dynamic costs. Taken together, these elements allow allows standard general-equilibrium channels to interact with energy transition and the geography of upstream clean-technology goods production, connecting to recent work on trade and the environment (Shapiro, 2021; Kortum and Weisbach, 2021; Xiang, 2023; Cruz and Rossi-Hansberg, 2024; Caliendo et al., 2024; Garcia-Lembergman et al., 2023; Farrokhi and Lashkaripour, 2024; Hsiao, 2024).

2 Background

2.1 Production and Trade in Renewable Energy Equipment

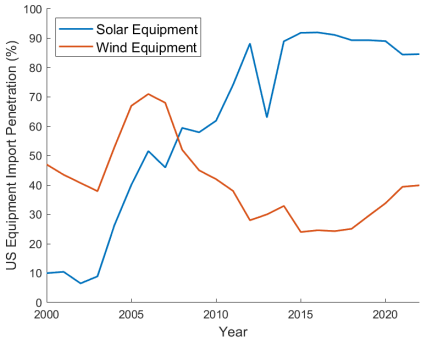
In this section, I present evidence of the prevalence of trade in renewable energy equipment by showing (a) the U.S. import penetration ratio for equipment and (b) the share of major countries

[3] For empirical evidence on within-country effects of energy-production subsidies, see Aldy et al. (2023); Gerarden (2023); De Groote and Verboven (2019); Gugler et al. (2021); Hitaj and Löschel (2019); Banares-Sanchez et al. (2024).

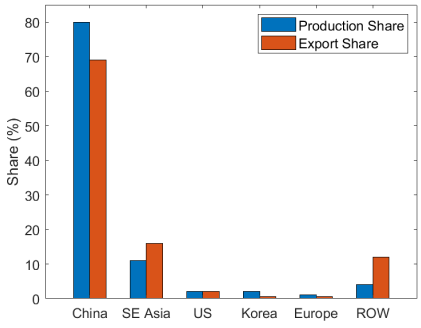
[4] Bollinger et al. (2024) study the impact of solar tariffs within the U.S. and explore the counterfactual effects of solar-equipment subsidies. My paper differs by focusing on the comparative global effects of energy and equipment subsidies using a dynamic general-equilibrium model that incorporates learning-by-doing in both solar and wind.

Figure 1: Trend in Equipment Trade, Production, and Price

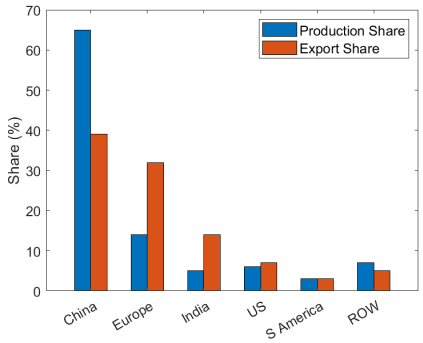
(a) US Import Penetration



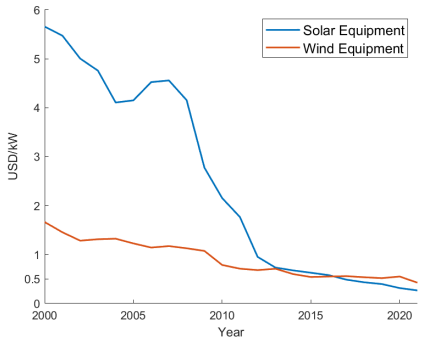
(b) Global Share in Solar Equip.



(c) Global Share in Wind Equip.



(d) Equipment Price



Note: Panel (a) depicts the import penetration ratio of US solar and wind equipment. Panel (b) depicts production share and export share of major countries in solar equipment, and panel (c) depicts production share and export share in wind equipment. Panel (d) plots the global price of solar and wind energy equipment from 2000 to 2021.

involved in the production and export of solar and wind energy equipment.[5]

Panel (a) in Figure 1 shows the time series of the import-penetration ratio of equipment in the U.S. from 2000 to 2022. The U.S. reliance on imports is more pronounced for solar energy equipment than for wind energy equipment. The import penetration ratio for solar equipment (blue solid line) was around 10% in 2000, but dramatically increased to 83% by 2022. The import penetration ratio for wind equipment (red solid line) also remained substantial, reaching 39% in 2022.

Panel (b) and (c) in Figure 1 show the shares of major countries in the production and export of solar and wind energy equipment in 2022. The production of renewable energy equipment is highly concentrated in a few countries, with China as the dominant player. In solar equipment, China accounts for 80 percent of global production and 69 percent of global exports, while Southeast Asian countries contribute 11 percent of production and 16 percent of exports. Other countries hold relatively small shares; for example, the U.S. accounts for 2 percent of both global production and

[5]For the details about data, see the Appendix section B.3.

exports.

In wind equipment, although China's dominance is less pronounced than in solar equipment, it still leads with 65 percent of global production and 39 percent of exports. European countries play a significant role, accounting for 14 percent of production and 32 percent of export shares. The U.S. accounts for 6 percent of global production and 7 percent of global exports.

2.2 Learning-by-doing in Renewable Energy Equipment

The costs of fossil fuels and nuclear power are primarily driven by two factors: the price of the fuel they consume and the plant's operating expenses. In contrast, the cost of electricity from renewable energy is mainly influenced by the price of the equipment required for its production.

The prices of renewable energy equipment, including both solar and wind equipment, have experienced significant declines since 2000. Panel (d) in Figure 1 shows the time series of prices for solar and wind energy equipment per kW from 2000 to 2021. The price of solar equipment (blue solid line) decreased by 95 percent over 21 years, from 5.6 US dollars per kW in 2000 to 0.27 US dollars per kW in 2021. The price of wind equipment (red solid line) also experienced a substantial price decline, dropping from 1.63 US dollars per kW in 2000 to 0.43 US dollars per kW in 2021, a 74 percent decrease. In the literature, this process has been understood through "learning-by-doing," which I adopt in this paper.[6]

Thanks to the large learning-by-doing effect in the renewable energy equipment, the price of electricity from solar and wind also has shown a dramatic decreasing pattern over time. Figure B.1 compares the price of electricity from various energy sources such as solar, wind, nuclear and coal with respect to cumulative installed capacity. While the price of solar (wind) electricity declined by 36% (23%) when doubling the installation, there is no such pattern observed in nuclear energy and coal.

3 Model

In this section, I construct a dynamic multi-country-multi-sector general equilibrium model to study the impact of green industrial policies on global welfare and carbon emissions. In particular, the static part of the model extends Caliendo and Parro (2015) by incorporating detailed energy production, and then it connects to the dynamic growth model with capital accumulation and external learning-by-doing in equipment production.

[6] See, for example, Baker et al. (2013), Bolinger et al. (2022), and Arkolakis and Walsh (2023). This paper's focus on learning-by-doing (LBD) also complements and contrasts with a parallel literature on Directed Technical Change, which models cost reductions as the result of R&D and innovation rather than cumulative production (e.g., Acemoglu et al. (2012), Acemoglu et al. (2016), and Donald (2024)). I use LBD because policies like the IRA are primarily aimed at scaling the domestic manufacturing and deployment of existing technologies, where cost declines are driven by cumulative production experience, rather than at incentivizing the invention of new technologies.

3.1 Environment

Consider a trade model with N countries indexed by $n = 1, \ldots, N$ and J sectors indexed by j. Time is discrete, $t = 1, \ldots, \infty$. Each country's economy consists of energy and non-energy sectors, with further sub-sectoral distinctions.

The model divides the economy into energy and non-energy sectors, further categorizing them into key sub-sectors. The energy sector includes three sub-sectors: solar (s), wind (w), and fossil fuel (f), collectively denoted by $\Omega_E = \{s, w, f\}$, where $\Omega_{RE} = \{s, w\}$ denotes the renewable energy sectors. The non-energy sectors include a capital goods sector (K) and a non-capital goods sector (O). The capital goods sector is subdivided into solar energy equipment (S), wind energy equipment (W), fossil fuel capital goods (F), and non-energy capital goods (D), with the set of all capital goods denoted by $\Omega_K = \{S, W, F, D\}$. Within this, the renewable energy equipment sector is $\Omega_{REE} = \{S, W\}$. The set of all sectors in the economy is $\Omega \equiv \Omega_E \cup \Omega_K \cup \Omega_O$, and Ω_j^* refers to the complement of sector j.

There is a continuum of intermediate goods $\omega^j \in [0, 1]$ in each sector j. The production process involves differentiated goods (ω^j) which are combined using a CES aggregator with an elasticity across varieties denoted as σ^j. The market structure is characterized by perfect competition.[7]

In each country n, the government can subsidize domestic production in the renewable energy and equipment sectors using an output price subsidy $s_{n,t}^j$, where $j \in \Omega_{REE} \cup \Omega_{RE}$. I assume the subsidies are financed by lump-sum tax from the household in each country.

3.2 Household

In each region n, the representative household is endowed with an initial stock of labor L_n and capital stocks $K_{n,1}^k$ for $k \in \Omega_K$. Labor is supplied inelastically and is mobile across sectors within each region. The representative household makes consumption decisions ($C_{n,t}^j$) and investment ($I_{n,t}^k$) decisions in each period to maximize lifetime utility. The household's utility is the discounted sum of consumption, weighted by Cobb-Douglas weights μ_n^j with disutility from carbon emissions factored into the utility function:

$$U_n = \sum_{t=1}^{\infty} \beta^{t-1} \log \Big[\prod_{j \in \Omega_K^*} (C_{n,t}^j)^{\mu_n^j} \frac{1}{1 + SCC_t(Z_t - Z_0)} \Big], \quad \text{where} \quad \sum_{j \in \Omega_K^*} \mu_n^j = 1. \tag{1}$$

The second term in square brackets captures the disutility from carbon. Z_0 is global emissions in the initial period from data and Z_t are global emissions in period t. SCC_t is a damage parameter, with a higher SCC_t indicating greater disutility from emissions. Following Shapiro (2021), carbon

[7] While both solar and wind equipment production is concentrated at the country level, this does not necessarily imply that individual firms possess market power. For example, major wind equipment producers such as Gamesa, Vestas, and Nordex reported negative profit margins (EBITDA) in 2022. (U.S. Department of Energy (2023))

emissions Z_t are a pure negative externality, which the household cannot directly choose.

3.3 Static Components

I begin by outlining the production and investment processes in the economy.

In the energy sector, the production of solar and wind energy requires a single input: installed solar and wind equipment, respectively. The production functions for both exhibit decreasing returns to scale. Fossil fuel production, on the other hand, requires a combination of fossil fuel capital, labor, and intermediate goods. Solar, wind, and fossil fuel are then aggregated using a nested CES technology to generate composite energy.

In the non-energy sector, production requires intermediate goods including composite energy, non-energy capital, and labor. The renewable energy equipment sector benefits from external learning-by-doing effects, resulting in dynamic economies of scale, where cumulative past production experience enhances current productivity. Once capital goods—such as solar and wind equipment, fossil fuel capital goods, and non-energy capital goods—are produced, they are traded across countries and accumulated as capital stock through investment. This investment process enables these capital goods to serve as inputs for future production.

Renewable Energy Production. Each renewable-energy sector j (solar and wind) in region n at time t is produced using installed equipment in each region with production efficiency $z_n^j(\omega^j)$:

$$y_{n,t}^j(\omega^j) \quad = \quad z_n^j(\omega^j)\left(K_{n,t}^j(\omega^j)\right)^{\xi_n^j}, \text{ for } j \in \Omega_{RE}. \tag{2}$$

The production efficiency $z_n^j(\omega^j)$ is country- and sector-specific, capturing heterogeneity in solar and wind potential across countries. ξ_n^j reflects within-country heterogeneity in solar and wind potential. The intuition is that as a country increases solar or wind equipment installations, areas with higher potential are utilized first, and additional installations are placed in locations with relatively lower potential *within* the country.

Then the unit cost is given by $\frac{c_{n,t}^j}{z_n^j(\omega^j)}$, where $c_{n,t}^j$ is a function of stock of capital and rental rate of capital in region n at time t.

$$c_{n,t}^j \quad = \quad \left(K_{n,t}^j\right)^{1-\xi_j} r_{n,t} \tag{3}$$

Due to the decreasing returns to scale, the unit cost of producing renewable energy rises as the stock of installed renewable equipment increases. Holding other factors constant, a country facing stronger decreasing returns to scale will experience a slower rate of energy transition and have a lower demand for renewable equipment.

Fossil Fuel Energy Production. Fossil fuel sector combines labor, fossil fuel capital, and interme-

diates in country n at time t:

$$y^f_{n,t}(\omega^f) \quad = \quad z^f_n(\omega^f)(L^f_{n,t}(\omega^f))^{\gamma^{L,f}_n}(K^F_{n,t}(\omega^f))^{\gamma^{F,f}_n}\prod_{j'=\Omega^*_K}\left(M^{j'f}_{n,t}(\omega^f)\right)^{\gamma^{M,j'f}_{n,t}} \tag{4}$$

where $L^j_{n,t}(\omega^f)$, $K^F_{n,t}(\omega^f)$, and $M^{j'j}_{n,t}(\omega^f)$ is the quantity of labor, fossil-fuel capital stock, and intermediate goods from sector j' used in country n, respectively. $\gamma^{L,f}_n$, $\gamma^{F,f}_n$, and $\gamma^{M,j'f}_{n,t}$ denotes the share of value added from each input for producing $y^f_{n,t}$, respectively. The production technology for fossil fuel energy features constant return to scale, *i.e.*, $\gamma^{L,f}_n + \gamma^{F,f}_n + \sum_{j'=\Omega^*_K}\gamma^{M,j'f}_{n,t} = 1$.

The unit cost is given by $\frac{c^f_{n,t}}{z^f_n(\omega^f)}$, where

$$c^f_{n,t} \quad = \quad B^f_{n,t}(w_{n,t})^{\gamma^{L,f}_n}(r_{n,t})^{\gamma^{F,f}_n}\prod_{j'=\Omega^*_K}\left(P^{j'}_{n,t}\right)^{\gamma^{M,j'f}_{n,t}} \tag{5}$$

Here $B^f_{n,t}$ is a function of share of value added from each inputs.[8]

Composite Energy Production. Composite energy input $e_{n,t}(\omega^e)$ in each country n is a CES composite between energy generated by solar, wind, and fossil fuel, but with a nested structure. In the inner nest, renewable energy, $y^r_{n,t}$ is a CES composite of solar and wind energies:

$$y^r_{n,t}(\omega^r) = \left[[\eta_r]^{\frac{1}{\rho}}[y^s_{n,t}(\omega^s)]^{\frac{\rho-1}{\rho}} + [1-\eta_r]^{\frac{1}{\rho}}[y^w_{n,t}(\omega^w)]^{\frac{\rho-1}{\rho}}\right]^{\frac{\rho}{\rho-1}} \tag{6}$$

where η_r is a level shifter and ρ captures substitution elasticity between solar and wind energies.

Then the composite energy $e_{n,t}(\omega^e)$ is CES composite of renewable energy and fossil fuel energy:

$$e_{n,t}(\omega^e) = \left[[\eta_e]^{\frac{1}{\psi}}[y^r_{n,t}(\omega^r)]^{\frac{\psi-1}{\psi}} + [1-\eta_e]^{\frac{1}{\psi}}[y^f_{n,t}(\omega^f)]^{\frac{\psi-1}{\psi}}\right]^{\frac{\psi}{\psi-1}}, \tag{7}$$

where η_e is a level shifter and ψ captures substitution elasticity between renewable energy and fossil fuel energy.

Due to the CES technology used in composite energy production, the share of each energy source, $\gamma^{M,j'f}_{n,t}$, where $j' \in \Omega_E$, is time-dependent and endogenously determined by the relative prices of energy sources. This implies that while the energy intensity of production in each country-sector is governed by the parameter $\gamma^{j,e}_n$—which is calibrated outside the model—the fossil fuel intensity of production in each economy is determined endogenously within the model.

Carbon Emissions. Carbon emissions are proportional to fossil use and accumulate over time; there

[8] In particular, $B^f_{n,t} = \left((\gamma^{L,f}_n)^{\gamma^{L,f}_n}(\gamma^{F,f}_n)^{\gamma^{F,f}_n}\prod_{j'=\Omega}(\gamma^{M,j'f}_{n,t})^{\gamma^{M,j'f}_{n,t}}\right)^{-1}$

is no abatement technology, so decarbonization occurs only via a higher renewable share in the energy nest.[9]

Non-energy Sectors Production. Production technology for non-energy sectors, $j \in \Omega_E^*$, combines labor, non-energy capital $K_{n,t}^D$, and intermediates in country n at time t:

$$y_{n,t}^j(\omega^j) = z_{n,t}^j(\omega^j)(L_{n,t}^j(\omega^j))^{\gamma_n^{L,j}}(K_{n,t}^D(\omega^j))^{\gamma_n^{D,j}}\prod_{j'=\Omega_K^*}\left(M_{n,t}^{j'j}(\omega^j)\right)^{\gamma_{n,t}^{M,j'j}}. \tag{8}$$

Again, I assume constant return to scale, *i.e.*, $\gamma_n^{L,j} + \gamma_n^{D,j} + \sum_{j'=\Omega_K^*}\gamma_{n,t}^{M,j'j} = 1$. Then the unit cost is given by:

$$c_{n,t}^j = B_{n,t}^j(w_{n,t})^{\gamma_n^{L,j}}(r_{n,t})^{\gamma_n^{D,j}}\prod_{j'=\Omega_K^*}\left(P_{n,t}^{j'}\right)^{\gamma_{n,t}^{M,j'j}} \text{ for } j \in \Omega_E^*, \tag{9}$$

where $B_{n,t}^j$ is a function of share parameters.[10]

For the equipment sectors, productivity $z_{n,t}^j$ for $j \in \Omega_{REE}$, is endogenously determined by learning-by-doing, with the exact specification provided in a later section (Section 3.4).

Composite Intermediate Goods. Composite intermediate goods in sector j are produced by aggregating a continuum of varieties using a standard Dixit–Stiglitz aggregator. The implied variety demand and sectoral price index are standard and reproduced in Appendix A.1. We retain only the notation $Q_{n,t}^j$ and $P_{n,t}^j$ in the main text.

Trade Costs and Prices. Trade in the outputs of tradable sectors incurs standard iceberg trade costs; κ_{ni}^j units of sector j good must be shipped from country i to n to deliver one unit, with $\kappa_{ii}^j = 1$. Combined with subsidies $s_{i,t}^j$, a unit cost of intermediate good ω^j produced in country i and available in country n is given by $c_{i,t}^j\kappa_{ni}^j(1-s_{i,t})/z_{i,t}^j(\omega^j)$. This implies that the price of intermediate good ω^j in country n is $p_{n,t}^j(\omega^j) = \min_i\left\{\frac{c_{i,t}^j\kappa_{ni}^j(1-s_{i,t}^j)}{z_{i,t}^j(\omega^j)}\right\}$.

I follow probabilistic representation of technologies in Eaton and Kortum (2002). That is, production efficiency is modeled as a realization of the random variable z_n^j , which follows a Fréchet distribution:

$$Pr[z_n^j(\omega^j) \le z] = \exp\{-A_n^j z^{-\theta^j}\}.$$

Here the location parameter A_n^j which is sector-country specific, governs the average productivity in each sector, and the shape parameter θ^j, which is sector-specific, captures the dispersion of produc-

[9] I do not consider abatement technologies that reduce carbon emissions while using the same amount of fossil fuel.

[10] $B_{n,t}^j = \left((\gamma_n^{L,j})^{\gamma_n^{L,j}}(\gamma_n^{D,j})^{\gamma_n^{D,j}}\prod_{j'=\Omega}(\gamma_{n,t}^{M,j'j})^{\gamma_{n,t}^{M,j'j}}\right)^{-1}$.

tivity across goods ω^j.[11] Then the price index for each sector j in country n is given by

$$P_{n,t}^j = \left[\sum_i (c_{i,t}^j (1 - s_{i,t}^j)\kappa_{ni}^j)^{-\theta^j} A_{i,t}^j\right]^{-1/\theta^j} \tag{10}$$

where $c_{i,t}^j$ is the unit production cost in origin i; $s_{i,t}^j \in [0,1)$ is an ad valorem output subsidy that lowers the producer's effective cost; and $\kappa_{ni,t}^j$ is an iceberg trade cost shipping from i to n with $\kappa_{ii,t}^j = 1$. I assume that all sectors are tradable except for renewable energy, *i.e.*, $\kappa_{ni}^s = \kappa_{ni}^w = \infty$ for $i \neq n$. This implies that for solar and wind energy, the price is given by $P_{n,t}^j = c_{n,t}^j (1 - s_{n,t}^j)(A_{n,t}^j)^{-1/\theta^j}$ for $j \in \Omega_{RE}$, and other countries' energy subsidies have no direct impact to renewable energy prices in country n. On the other hand, as equipment is tradable, equipment subsidy in one country affects other countries' equipment prices through trade.

Due to the CES structure, the share of fossil fuel input in producing goods in sector j, denoted by $\gamma_{n,t}^{M,fj}$, is endogenously determined by the following equation:[12]

$$\gamma_{n,t}^{M,fj} = \gamma_{n,t}^{M,Ej}\left[1 + \frac{\eta_e}{1-\eta_e}\left(\frac{P_{n,t}^f}{P_{n,t}^r}\right)^{\psi-1}\right]^{-1}. \tag{11}$$

An energy subsidy lowers the domestic price of non-tradable renewables $P_{n,t}^r$, narrowing the renewable–fossil wedge. By the energy CES share relation (equation (11)), when the substitution elasticity $\psi > 1$ this raises the renewable share and reduces domestic emissions. However, this domestic action triggers two international spillovers: (i) higher home-market demand for tradable equipment increases pressure on the global equipment price, potentially slowing others' transitions; (ii) reduced domestic fossil fuel use depresses the world fossil price, inducing carbon leakage abroad as foreign users substitute toward fossil fuel.

Trade share. Trade flows are the fraction of country n's expenditure on sector j goods produced by country i. Under the Fréchet draws, expenditure shares are

$$\pi_{ni,t}^j = \frac{\left(c_{i,t}^j (1 - s_{i,t}^j)\kappa_{ni}^j\right)^{-\theta^j} A_{i,t}^j}{\sum_m \left(c_{m,t}^j (1 - s_{m,t}^j)\kappa_{nm}^j\right)^{-\theta^j} A_{m,t}^j} \tag{12}$$

An equipment subsidy by exporter n raises foreign buyers' import shares of n's equipment. For any $m \neq n$ and equipment sector k, $\frac{\partial \pi_{mn,t}^k}{\partial s_{n,t}^k} > 0$, as implied by the trade-share system (12).

Because equipment is tradable, a higher $\pi_{mn,t}^k$ increases shipments from n to m, thereby raising exporter n's cumulative output in sector k. With country-specific learning-by-doing (introduced later

[11] Following Caliendo and Parro (2015), I assume the distributions of productivities are i.i.d across goods, sectors, countries, and time. Furthermore, assume $1 + \theta^j > \sigma^j$.

[12] Analogous expressions for the shares of other energy inputs for production and consumption follow directly from the same CES aggregator; see Appendix A.2 for the general derivation.

in equation (19)), this accelerates n's future productivity growth and lowers its costs, which passes through into lower delivered equipment price indices $P^k_{m,t+\ell}$ abroad and, via cheaper installations, lower renewable energy prices $P^r_{m,t+\ell}$ over time. By contrast, a renewable-energy subsidy $s^r_{n,t}$ acts on a non-tradable good in our setting, so this cross-border reallocation channel is absent.

Lastly, from (12) the magnitude of the effect scales with the trade elasticity θ^k: higher θ^k amplifies the response of global market shares to a given price change induced by $s^k_{n,t}$.

Total Expenditure. I denote country n's total absorption in sector j by $x^j_{n,t}$, and country m's absorption in sector j from country n by $x^j_{mn,t}$, such that $x^j_{m,t} = \sum_n x^j_{mn,t}$. Additionally, the value of country n's total expenditure in sector j is defined as $X^j_{n,t} = P^j_{n,t} x^j_{n,t}$. Let $Y^j_{n,t}$ denote the gross production value in country n's sector j at time t. Then,

$$Y^j_{n,t} = \sum_{m=1}^{N} \frac{\pi^j_{mn,t}}{1 - s^j_{m,t}} X^j_{m,t}. \tag{13}$$

Equation (13) shows that gross output in country n's sector j is equal to the sum of total exports and domestic sales, net of subsidy.

Let the final household spending on each sector in country n be defined as $X^{F,h}_{n,t} = P^h_{n,t} C^h_{n,t}$ for $h \in \Omega^*_K$, and $Xn, t^{F,k} = P^k_{n,t} I^k_{n,t}$ for $k \in \Omega_K$. Total expenditure on sector j is then the sum of the use of sector j's output as intermediates across sectors j', and the final spending on sector j in country n:

$$X^j_{n,t} = \sum_{j' \in \Omega} \gamma^{M,j'j}_n \gamma^{j'}_n Y^{j'}_{n,t} + X^{F,j}_{n,t}. \tag{14}$$

Market Clearing. The labor market clearing condition for country n implies that labor income equals value added across sectors:

$$w_{n,t} L_{n,t} = \sum_{j \in \Omega} \gamma^{L,j}_n Y^j_{n,t}. \tag{15}$$

Similarly, the capital market clearing condition implies that capital income equals the value added of capital across sectors:

$$\sum_{k \in \Omega_K} r_{n,t} K^k_{n,t} = Y^s_{n,t} + Y^w_{n,t} + \gamma^{F,f}_n Y^f_{n,t} + \sum_{j \in \Omega^*_E} \gamma^{D,j}_n Y^j_{n,t}. \tag{16}$$

Note that the capital share in the production of solar and wind energy is one, meaning it relies entirely on capital inputs. In contrast, fossil fuel capital goods are exclusively used in fossil fuel energy production.

Trade Balance. Let D_i denote the aggregate trade deficit in country i. Using Equation (14), we have

$$\sum_{j\in\Omega}\sum_{n=1}^{N}\frac{\pi_{in,t}^{j}}{1-s_{i,t}^{j}}X_{i,t}^{j}-D_{i,t}=\sum_{j\in\Omega}\sum_{i=1}^{N}\frac{\pi_{ni,t}^{j}}{1-s_{n,t}^{j}}X_{n,t}^{j}. \tag{17}$$

The left-hand side of equation (17) represents country i's total expenditure, net of subsidies, minus its trade deficit, D_i. The right-hand side sums country i's exports, net of tariffs, across all sectors j. I assume trade is balanced at the global level: the total trade deficits across all countries sum to zero, $\sum_i D_{i,t} = 0$, and each country's aggregate trade deficit is treated as exogenous. However, this framework allows sectoral trade deficits to be endogenously determined, enabling the model to capture the impact of changes in trade surpluses or deficits within the renewable energy equipment sector due to the subsidies.

3.4 Dynamic Components

Capital Accumulation. Capital evolves with convex installation costs as

$$K_{n,t+1}^{k}=\chi_k\left(\frac{I_{n,t}^{k}}{K_{n,t}^{k}}\right)^{\alpha}(K_{n,t}^{k})^{1-\alpha}+(1-\delta^{k})K_{n,t}^{k},\qquad k\in\Omega_K, \tag{18}$$

where $\chi_k > 0$ scales installation efficiency, $\alpha \in (0,1)$ governs adjustment costs—so installation efficiency declines in $I_{n,t}^{k}/K_{n,t}^{k}$ (Eaton et al., 2016; Ravikumar et al., 2019)—and $\delta^k \in (0,1)$ is depreciation. Investment equals purchases of capital good k by the representative household: $I_{n,t}^{k} = x_{n,t}^{k}$.

Learning-by-doing in Renewable Energy Equipment Production. In this model, cumulative past output drives current productivity in equipment production. A key assumption is that learning occurs within each country and is external to the firms in the sector.[13] The productivity of region n in producing renewable energy equipment $k \in \Omega_{REE}$ at time t, denoted by $A_{n,t}^{k}$, is determined by the cumulative production in each country:

$$A_{n,t}^{k}=\nu^{k}\Big(\sum_{i=1}^{t-1}(\mu)^{i}y_{n,t-i}^{k}\Big)^{\nu_D^{k}}. \tag{19}$$

Here, ν^k is a sector-specific shifter, $\mu < 1$ represents the forgetting rate, and ν_D^k governs the learning rate. This ensures that productivity does not grow indefinitely, allowing the model to remain well-behaved and reach a steady state.

[13] From a modeling perspective, incorporating global spillovers, as in Arkolakis and Walsh (2023), or spillovers across solar and wind equipment technologies, as in Donald (2024), is straightforward. However, I find no empirical evidence of significant global spillovers in the data, as discussed in Section 4.4. In Appendix Section C.10, I examine the scenario with frictionless global spillovers in learning-by-doing as a robustness check.

This country-specific learning-by-doing framework emphasizes how subsidies shape dynamic comparative advantage. An equipment subsidy in the U.S. raises domestic output today, which lifts future productivity via learning-by-doing; conversely, lower output abroad reduces others' scope for learning, affecting cross-country productivity gaps over time.

Household Optimality. The household's within-period budget constraint is

$$\sum_{h\in\Omega_K^*} P_{n,t}^h C_{n,t}^h = w_{n,t}L_{n,t} + \sum_{k\in\Omega_K} r_{n,t}^k K_{n,t}^k - \sum_{j\in\Omega} \frac{s_{n,t}^j}{1-s_{n,t}^j} \sum_{m=1}^{N} \pi_{mn,t}^j X_{m,t}^j + D_{n,t} - \sum_{k\in\Omega_K} P_{n,t}^k I_{n,t}^k \quad \equiv \quad E_{n,t},$$

where the left-hand side is expenditure on non-capital consumption goods. The right-hand side collects labor income $w_{n,t}L_{n,t}$, capital income $\sum_k r_{n,t}^k K_{n,t}^k$, subtracts the government's subsidy outlays in n (the term with $s_{n,t}^j$), adds trade deficit $D_{n,t}$, and subtracts investment spending. Thus $E_{n,t}$ denotes disposable expenditure available for consumption in period t.

Given prices and $E_{n,t}$, the household's within-period allocation across $h \in \Omega_K^*$ satisfies

$$P_{n,t}^h C_{n,t}^h \;=\; \mu_n^h \, E_{n,t}. \qquad h \in \Omega_K^*, \tag{20}$$

To characterize investment, define period utility as

$$u_t(C_{n,t}) \equiv \log C_{n,t} + \log\Big(\tfrac{1}{1+SCC_t(Z_t-Z_0)}\Big), \quad C_{n,t} \equiv \prod_{j\in\Omega_K^*} (C_{n,t}^j)^{\mu_n^j},$$

and let $P_{n,t}$ denote the corresponding consumption price index, $P_{n,t} \equiv \prod_{j\in\Omega_K^*}^{J} \left(\frac{P_{n,t}^j}{\mu_n^j}\right)^{\mu_n^j}$. The capital-accumulation equation (18) implies the Euler condition, for each $k \in \Omega_K$:[14]

$$\frac{u_t'(C_{n,t})}{u_{t+1}'(C_{n,t+1})} \frac{P_{n,t+1}}{P_{n,t}} \frac{p_{n,t}^k}{\chi_k} \left(\frac{I_{n,t}^k}{K_{n,t}^k}\right)^{1-\alpha} = \beta\alpha \left[r_{n,t+1}^k + \frac{(1-\alpha)\, p_{n,t+1}^k I_{n,t+1}^k}{\alpha K_{n,t+1}^k} + \frac{(1-\delta^k)\, p_{n,t+1}^k}{\alpha\chi_k} \left(\frac{I_{n,t+1}^k}{K_{n,t+1}^k}\right)^{1-\alpha} \right]. \tag{21}$$

The left-hand side is the marginal installation cost at t of delivering an additional unit of effective capital at $t+1$; the right-hand side is the discounted marginal payoff at $t+1$ (the rental return plus continuation value from capital and adjustment). An equipment subsidy reduces the equipment cost $p_{n,t}^k$, lowering the marginal cost of investment and therefore raising desired investment in renewable equipment relative to other capital goods. Combined with the capital law of motion (eq. (18)), this implies higher installation along the transition path and faster accumulation of renewable equipment capital.

Steady State. In steady state, productivities A_n^k and capital stocks K_n^k are constant. The Euler equations (21) and the accumulation law (18) pin down (i) the investment–capital ratio for each k

[14] If $\alpha = 1$ and $\chi_k = 1$, this collapses to $\frac{u_t'(C_{n,t})}{u_{t+1}'(C_{n,t+1})} \frac{P_{n,t+1}}{P_{n,t}} P_{n,t}^k = \beta\big[r_{n,t+1}^k + (1-\delta^k)P_{n,t+1}^k\big]$.

and (ii) the ratio of rental payments to investment spending:

$$\frac{I_n^k}{K_n^k} = \left(\frac{\delta^k}{\chi_k}\right)^{1/\alpha}, \qquad \frac{r_n^k K_n^k}{p_n^k I_n^k} = \frac{1-\beta+\beta\delta^k\alpha}{\beta\delta^k\alpha},$$

where other endogenous values under the steady state follow the equilibrium conditions.

Welfare. Welfare in each country n is defined as the discounted sum of utility, which can be represented by real income, adjusted to incorporate the disutility from carbon emissions:

$$W_n = \sum_{t=1}^{\infty} \beta^{t-1} \log\left(\frac{E_{n,t}}{P_{n,t}} \frac{1}{(1+SCC_t(Z_t - Z_0))}\right). \tag{22}$$

3.5 Dynamic General Equilibrium

Definition 1 summarizes the equilibrium conditions.

Definition 1. ***A sequential equilibrium of the model*** *is a set of prices* $\left\{w_{n,t}, P_{n,t}^j, r_{n,t}^k\right\}_{n=1,j=1,k=1,t=1}^{N,J,K,T}$ *and allocations of goods and labor* $\left\{\pi_{ni,t}^j, L_{n,t}^j\right\}_{n=1,i=1,j=1,t=1}^{N,N,J,T}$ *that satisfies the static equilibrium conditions: production (equations* (2)-(9)*), trade shares (12), local prices (10), labor and market clearing conditions (equations* (15) *and* (16)*), and trade balance (17), and dynamic conditions: law of motion of capitals (18), and Euler equation (21).*

In the Appendix D, I show the numerical algorithm to solve this model.

3.6 From Mechanisms to Quantification

The model's open-economy structure, with traded equipment and *country-specific* learning-by-doing, generates distinct transmission channels for the energy subsidy and the equipment subsidy.

With renewable energy non-tradable and equipment tradable, the price system in (10)–(12) implies that energy subsidies shift only the domestic renewable–fossil wedge (via (11)), whereas equipment subsidies transmit internationally through delivered equipment prices and trade shares. Combined with the accumulation and Euler conditions (18)–(21), these price and share movements reallocate cumulative production across countries and—via learning-by-doing (19)—reshape future productivities.

These channels reveal a fundamental policy trade-off. The energy subsidy concentrates abatement domestically but risks negative price spillovers for the rest of the world. The equipment subsidy generates positive price spillovers through trade but does so by distorting the global geography of production at the expense of incumbent exporters. The ultimate impact on U.S. welfare, global welfare, and total carbon emissions is therefore theoretically ambiguous. The outcome depends on the

relative strength of these competing forces, governed by key parameters such as sectoral trade elasticities θ^j, the elasticity of substitution between energy sources ψ, learning-by-doing rates ν_D^k, and renewable energy potential A_n^r. This highlights the necessity of a quantitative evaluation to determine the magnitude and net direction of these effects, to which we now turn.

4 Calibration and Model Validation

4.1 Countries and Sectors Covered

Using the OECD Input–Output data, I aggregate the dataset into 12 countries and 6 regions, including the EU, Southeast Asia, South America, Africa, the Middle East, and the rest of the world. Appendix Section B.2 shows the list of countries. For sectors, I aggregate into 10 categories: 3 energy sectors, 3 energy equipment sectors, and 4 additional sectors (Agriculture & Mining, Non-Durable Manufacturing, Durable Manufacturing, and Services).

4.2 Parameters in Renewable Energy Production

Data. I utilize (i) geospatial resource potentials from the Global Solar and Wind Atlases measured in kWh/m^2, (ii) renewable power plant locations from the Global Solar and Wind Power Trackers ($\geq$10MW; $\approx$70% of global capacity), and (iii) a Development Potential Index (DPI) from Oakleaf et al. (2019) summarizing siting feasibility (physical and social constraints).[15]

Measuring the absolute-advantage parameter A_n^r. A_n^r captures cross-country heterogeneity in renewable potential. Countrywide averages of atlas potentials overweight infeasible sites, so I compute $A_{n,1}^r$ using the *atlas–tracker matched* sample: the average resource potential at actual solar and wind plant sites installed up to 2021 (the initial calibration year). Specifically, I calculate the average renewable potential at the sites of solar and wind farms installed up to 2021, which serves as the initial period for the quantitative analysis.[16] Panel (a) of Figure B.3 reports the cross-country distribution.

Measuring decreasing returns, ξ_n^r. Within-country heterogeneity implies progressively lower-quality sites as deployment expands. Using DPI-weighted potential distributions, I construct each country's "resource supply curve" (best-to-marginal sites) and estimate its local slope around observed deployment, which I map into $\xi_n^r < 1$ via the elasticity of unit cost with respect to installed capacity in (3). Intuitively, lower ξ_n^r steepens marginal cost growth, slowing the transition and raising the value of equipment efficiency gains. Panel (b) of Figure B.3 shows estimates; the means are $\xi^s = 0.965$ (sd 0.004) and $\xi^w = 0.954$ (sd 0.007), indicating stronger DRS and greater dispersion for wind.

In Appendix Section B.5.2, I also use an alternative measure to compute the decreasing returns

[15] Details are documented in Appendix B.5.1.

[16] Further details on the dataset are provided in Appendix Section B.5.2.

to scale by measuring the relationship between each renewable potential and installed renewable energy capital stock. The result (Table B.2) shows that the change in capital stocks is also strongly negatively correlated with change in the renewable potential, confirming the decreasing returns to scale.

4.3 Estimating CES in Energy Production

Energy production in the model is a two–level CES. I estimate the *inner-nest* elasticity between solar and wind, ρ, directly from the model-implied log–log relationship

$$\log\left(\frac{y^s_{n,t}}{y^w_{n,t}}\right) = -\rho \log\left(\frac{p^s_{n,t}}{p^w_{n,t}}\right) + FE_n + \lambda t + \varepsilon_{n,t}, \tag{23}$$

where FE_n absorb time-invariant cross-country heterogeneity (e.g., average site quality, grid mix, permitting) and λt captures common technological progress. Equation (23) corresponds to the demand system dual to the inner CES aggregator in (6).

Relative prices and quantities are jointly determined, so OLS is biased by simultaneity and measurement error in prices. To address this, I instrument $\log(p^s_{n,t}/p^w_{n,t})$ with wind subsidies that vary across country–year. The relevance of this instrument aligns with the presence of decreasing returns to scale in renewable energy, where subsidies directly affect unit costs. The exclusion restriction assumes that renewable energy subsidies influence electricity demand only through their impact on relative price differences.[17]

Data. The data on solar and wind energy output (y^s, y^w) comes from the International Renewable Energy Agency (IRENA). For solar and wind energy prices, I construct price data for 20 countries by combining the levelized cost of electricity (LCOE) for solar and wind (sourced from IRENA) with wind energy subsidies (from OECD) for the years 2010-2021.

Results. Table 1 reports estimates. OLS suggests an elastic response to relative prices; adding FE_n and trends attenuates the slope as expected. The preferred IV with FE+trend delivers $\hat{\rho} = 0.712$, rejecting perfect substitutability which is commonly held assumption in the literature. The weak substitution between solar and wind energy can be attributed to the intermittency issues associated with both energy sources (Gentile (2024)). A 10% fall in the solar–to–wind price ratio is associated with a 7.1% rise in the solar–to–wind output ratio, holding fixed effects and the common trend constant. This ρ pins down how quickly the renewable composite rebalances internally in response to relative cost shocks (e.g., targeted subsidies, equipment price movements) and, through the outer nest, how those shocks propagate to the fossil share via (11).

Outer nest. For substitution between the renewable composite and fossil, I set $\psi = 3.08$ from Jo

[17] Institutionally, feed-in tariffs/premia and production tax credits are set by policy processes with lags and are not mechanically tied to short-run demand conditions. This supports the exclusion restriction that subsidies affect $\log(y^s/y^w)$ only through $\log(p^s/p^w)$. Moreover, wind energy subsidies are frequently part of broader, long-term renewable energy strategies rather than reactive policies to short-term demand fluctuations.

Table 1: Estimates for Substitution Elasticity (Inner Nest)

	Dependent Variable: $\ln(y^s_{n,t}/y^w_{n,t})$			
	(1) OLS	(2) FE	(3) FE+Trend	(4) IV FE+Trend
$\ln(p^s_{n,t}/p^w_{n,t})$	-1.067	-1.173	-0.403	-0.712
	(0.211)	(0.156)	(0.188)	(0.401)
1st Stage F				88.16
F-stat	25.56	56.19	54.00	14.69
N	144	144	144	144
FE		✓	✓	✓
Trend			✓	✓
IV				✓

(2023), within the range reported by Papageorgiou et al. (2017) and Wiskich (2023). Intuitively, renewables mostly supply on-grid electricity, while fossil inputs have broader end uses (e.g., internal combustion engines), rationalizing $\psi < \infty$.[18]

4.4 Estimating Learning Rate of Equipment Production

To calibrate learning-by-doing (LBD) in renewable equipment, I estimate the elasticity of productivity with respect to cumulative domestic output. Guided by (19), the estimating equation is

$$\log A^j_{n,t} = \nu^j_D \log\Big(\sum_{s=1}^{t-1} \mu^s y^j_{n,t-s}\Big) + \nu^j_G \log\Big(\sum_{i\neq n}\sum_{s=1}^{t-1} \mu^s y^j_{i,t-s}\Big) + \nu^j_n + \lambda t + u^j_{n,t}, \qquad j \in \Omega_{REE},$$

where $y^j_{n,s}$ is the output of renewable energy equipment j in country n at time s and μ is the forgetting rate, which I set $\mu = 0.99$ following Arkolakis and Walsh (2023). The term $(\sum_{i\neq n}\sum_{s=1}^{t-1} y^j_{i,s})$ captures the global cumulative output, excluding country n. Identification in this specification relies on within-country variation, while controlling for global spillover effects and common technological progress over time.

Recovering $A^j_{n,t}$ by inversion. To run this regression, I first need to recover the time-series data for renewable energy equipment productivity across countries ($A^j_{n,t}$). I infer productivity paths $\{A^j_{n,t}\}$ using the trade share equation,

$$\pi^j_{nn,t} = A^j_{n,t}\left(\frac{c^j_{n,t}}{P^j_{n,t}}\right)^{-\theta^j}, \tag{24}$$

where $\pi^j_{nn,t}$ is the domestic expenditure share, $c^j_{n,t}$ the input cost bundle, $P^j_{n,t}$ the sectoral price index, and θ^j the trade elasticity. Given (π, c, P, θ), I back out $A^j_{n,t}$. Data construction is summarized here and detailed in Appendix B.4: (i) $c^j_{n,t}$ combines wages, manufactured inputs, and services from Penn

[18] Robustness to higher $\psi = 5$ is reported in Appendix C.10; the main comparative statics are unchanged, though the share response in (11) scales proportionally.

Table 2: Estimating Learning-by-Doing in Equipment Production

	Solar ($\ln A^S_{n,t}$)			Wind ($\ln A^W_{n,t}$)		
	(1)	(2) FE	(3) FE+Trend	(4)	(5) FE	(6) FE+Trend
$\ln\left(\sum_{s=1}^{t-1} y^S_{n,s}\right)$	1.406***	1.301***	1.261***			
	(0.126)	(0.294)	(0.301)			
$\ln\left(\sum_n \sum_{s=1}^{t-1} y^S_{n,s}\right)$			-0.592			
			(0.915)			
$\ln\left(\sum_{s=1}^{t-1} y^W_{n,s}\right)$				0.315***	0.263***	0.765***
				(0.0347)	(0.117)	(0.152)
$\ln\left(\sum_n \sum_{s=1}^{t-1} y^W_{n,s}\right)$						-0.985
						(0.673)
F-stat	125.2	126.4	83.95	82.34	26.41	27.54
N	119	119	119	190	190	190
FE		✓	✓		✓	✓
Trend			✓		✓	✓

Standard errors in parentheses. $^{*}p < 0.10$, $^{**}p < 0.05$, $^{***}p < 0.01$.

World Table 10.1; (ii) for solar, $\pi^S_{nn,t}$ uses PVPS output and price with Comtrade exports; (iii) for wind, I proxy absorption using IRENA annual installations and average installed cost, then combine with Comtrade trade flows to recover historical $\pi^W_{nn,t}$ and output.

Results. Table 2 reports estimates. For the preferred specification with FE and a time trend yields $\hat{v}^S_D = 1.261$ and $\hat{v}^W_D = 0.765$ for domestic LBD, whereas the corresponding global spillover terms are not statistically significant. The pattern—strong domestic LBD with limited global spillovers—is consistent with country-specific learning emphasized in the model.[19]

From $\hat{v}^j_D$ to learning rates. Taking logs of (24) and differentiating, the (partial) elasticity of price with respect to cumulative output is $\frac{\partial \ln P^j_{n,t+1}}{\partial \ln \sum_{s\le t} y^j_{n,s}} = -\frac{v^j_D}{\theta^j}$. Therefore, the implied "learning rate" (percent price decline for a doubling of cumulative output) is $LR^j = 1 - 2^{-v^j_D/\theta^j}$. Using the trade elasticities specified in the next section, $\theta^S = 4.76$ and $\theta^W = 2.51$, the preferred estimates imply $LR^S \approx 0.17$ and $LR^W \approx 0.19$, in line with the lower end of the empirical range for solar and the mid–range for wind.[20,21] These magnitudes imply that policies shifting demand toward a country's equipment sector can meaningfully steepen subsequent price declines, strengthening the dynamic

[19] One potential reason the estimates in this paper differ from those in the existing literature is that prior studies examine global- or firm-level learning rates, whereas I focus on country-level learning. When using globally aggregated data as in Arkolakis and Walsh (2023), estimates are primarily driven by prices and quantities in China, since most output originates there. Firm-level studies may yield different estimates from country-level analyses, depending on the magnitude of inter-firm spillover effects. Covert and Sweeney (2024) finds that while the inter-firm spillover effect in this sector is small, it is not negligible.

[20] v^S/θ^S = 1.261/ 4.762 = 0.264 and v^W/θ^W = 0.765 / 2.509 = 0.304. Then, the learning rate can be computed by $1 - 2^{-v^S/\theta^S} = 0.17$ and $1 - 2^{-v^W/\theta^W} = 0.19$.

[21] See Baker et al. (2013) (survey), Bolinger et al. (2022) (US: 24% solar, 15% wind), and Covert and Sweeney (2024) (wind: 14–29%).

Table 3: Trade Elasticities (θ^j)

Sectors	**Trade Elasticity** (θ^j)
Solar Energy	4.55
Wind Energy	4.55
Fossil Fuel	15.08
Solar Equipment	4.76
Wind Equipment	2.51
Agriculture and Mining	8.11
Non-Durable Manufacturing	4.55
Durable Manufacturing	5.26
Service	4.55

channel discussed in Section 3.6.

4.5 Trade Elasticities

Trade elasticities (θ^j) discipline how strongly delivered-price changes from policies reallocate expenditure across suppliers within each sector. I calibrate θ^j to product- or sector-level estimates.

Equipment sectors (solar, wind). For solar and wind equipment I use product-level elasticities from Fontagné et al. (2022), mapped via HS codes that most closely match the model's sectors. I take the estimates of HS4 codes associated with photovoltaic devices and wind-generating sets, yielding $\theta^S = 4.76$ and $\theta^W = 2.51$.[22] The relatively higher θ^S versus θ^W implies that an equal ad-valorem equipment subsidy generates a larger shift in global market shares in solar equipment than in wind, magnifying the trade-share channel and the learning-by-doing amplification discussed in Section 3.6.

Other tradable sectors. For broader aggregates I adopt estimates from multi-sector Eaton–Kortum calibrations: agriculture 8.11, durable manufacturing 5.26, non-durables 4.55, services 4.55, and fossil fuels 15.08, matched from Parro (2013) and Caliendo and Parro (2015).

Non-traded energy (solar, wind). Although solar and wind *energy* are non-tradable in the baseline ($\kappa = \infty$ across borders), θ^j still governs within-country variety dispersion in the sectoral price index. I set $\theta^s = \theta^w = 4.55$ which is the average elasticity in Caliendo and Parro (2015).

4.6 Other Parameter Values and Initial Values

Shares of inputs in production and consumption. Using OECD Input–Output data, I calibrate the shares of labor, capital, and intermediate goods (including composite energy) in production and consumption. For each sector, input shares are measured as payments to labor, capital, and intermediates

[22] Solar equipment: HS 8541 (photosensitive semiconductor devices, incl. PV cells); wind equipment: HS 8502 (electric generating sets and rotary converters).

divided by gross output. A challenge is that the dataset does not separately report labor vs. capital value added. Following Greenwood et al. (1997), I assume a capital share of 0.3 in value added to split the total. For the final-goods consumption share μ_n^j, I subtract intermediate expenditures from total expenditures in sector j and divide by total absorption.

Depreciation rates (δ_k). Following Arkolakis and Walsh (2023), I set the annual depreciation rates to $\delta_S = \delta_W = 0.03$, $\delta_F = 0.02$, and $\delta_D = 0.07$.

Capital adjustment cost (α) and investment efficiency (χ_k). Following Ravikumar et al. (2019), I set $\alpha = 0.76$ and $\chi_k = (\delta_k)^{1-\alpha}$.[23] Under this formulation, there are no adjustment costs in the steady state when investment just replaces depreciation.

Trade costs (κ_{ni}^j). To calibrate iceberg trade costs, I invert bilateral trade data under symmetric costs, $\kappa_{ni}^j = \kappa_{in}^j$, following Head and Ries (2001):

$$\kappa_{ni}^j = \left(\frac{X_{ni,t}^j \, X_{in,t}^j}{X_{nn,t}^j \, X_{ii,t}^j} \right)^{-\frac{1}{2\theta^j}}.$$

This uses the trade elasticity θ^j from Section 4 and observed bilateral expenditures $X_{ni,t}^j$ where $t =$ 2021.

Initial sector–region productivity (A). For all sectors except renewable energies, I recover initial productivities by inverting the model using (24). For solar and wind energy, I use the calibrated values based on renewable resource data in Section 4.2. A sector-specific level shifter in renewable energy aligns this sector's productivity with others to match the observed global share of renewables in primary energy consumption.

Discount factor (β). Each model period is a year; I set $\beta = 0.96$.

Damage parameter (SCC_t). I calibrate a time-varying social cost of carbon path consistent with EPA (2023): \$175/tCO_2e in 2021, \$206 in 2030, \$283 in 2050, and \$382 in 2080. I set $SCC_t =$ \$382 for $t >$ 2080. This schedule scales the flow disutility from cumulative emissions in (1).[24]

Initial labor and capital stocks (L, K). Initial labor is the total number of employed workers from the Penn World Table (variable `emp`). The construction of initial capital stocks by asset type is detailed in Appendix B.6.

Table 4 summarizes parameter values and their sources or calibration methods.

[23] $\alpha = 0.76$ corresponds to the annualized adjustment-cost parameter in Eaton et al. (2016).

[24] Country-heterogeneous social costs of carbon can be incorporated; Appendix B.7 outlines the implementation. Appendix C.10 reports sensitivity of the results with heterogeneous $SCC_{n,t}$.

Table 4: Parameter Values

	Parameters	Values	Source or Method
(Renewable)			
ξ	Decreasing returns to scale	Region-energy specific	Measuring slope using data from Oakleaf et al. (2019)
ρ	(Inner nest) CES elasticity of substitution	0.712	Estimation
ψ	(Upper nest) CES elasticity of substitution	3.08	Jo (2023)
μ	Forgetting rate in learning-by-doing	0.99	Arkolakis and Walsh (2023)
		(solar, wind)	
ν_D	LBD elasticity of renewable equipment production	(1.261, 0.765)	Estimation
(Other Parameters)			
A	Region-sectoral productivity	Region-sector specific	Renewable Potentials: see manuscript Other sectors: Model inversion using Equation (24)
θ^j	Trade elasticities	Sector-specific	Caliendo and Parro (2015) and Fontagné et al. (2022)
γ^L	Share of labor in production	Region-sector specific	Calibrated using OECD IO
γ^j	Share of intermediate goods in production	Region-sector specific	Calibrated using OECD IO
γ^F	Share of fossil fuel capital in production	Region-sector specific	Calibrated using OECD IO
γ^D	Share of non-energy capital in production	Region-sector specific	Calibrated using OECD IO
μ^j	Consumption share	Region-sector specific	Calibrated using OECD IO
β	Discount rate	0.96	
SCC_t	Damage parameter	Time-specific	Match social cost of carbon path of EPA (2023)
κ	Trade cost	Region-sector-pair specific	Head and Ries (2001)
(Capital)			
χ_k	Investment efficiency	$\delta_k^{1-\alpha}$	Ravikumar et al. (2019)
		(solar, wind, fossil, non-energy)	
δ^j	Depreciation rate	(0.03, 0.03, 0.02, 0.07)	Arkolakis and Walsh (2023)

4.7 Model Validation

Panel (a) of Table 5 lists the moments targeted in calibration. I match trade shares (the import share in domestic absorption) for all tradable sectors, while assuming the renewable energy sectors are non-tradable.[25] The model exactly matches China's shares of global solar and wind equipment production—82% and 65%, respectively. I also calibrate a level shifter in renewable energy production so that the model replicates the global renewable share in primary energy consumption (14%) in Energy Institute (2024).[26]

I then assess the model against non-targeted moments. First, I compare the share of equipment in global GDP in 2021; this moment both scales the budget impact of subsidies and disciplines the policy multipliers. The first row of Panel (b) in Table 5 shows a small gap between model and data.

A second non-targeted moment is the renewable energy share by country. This moment is informative because the key drivers—country-specific renewable potential and the DRS parameter—are measured outside the model. For 2021 (the initial year), the correlation between model outcomes and data across countries is 0.66. Panel (a) of Figure 2 plots model vs. data and shows a good fit.

To validate dynamics—how policy shapes equipment production over time—I examine whether the IRA simulation reproduces the observed rise in U.S. solar module production capacity. The latest data include capacity through 2024, two years after the IRA's passage (Wood Mackenzie, 2024). Panel (b) of Figure 2 compares the model's domestic market share for U.S. solar equipment, $\pi^{S}_{US,US}$ (solid blue), with an empirical series (red dashed).[27] The model captures the upward trend: U.S. domestic share rises from 14% in 2021 to 68% in 2024, compared with a 60% realized share. The simulated response is somewhat faster, reflecting the annual timing in the model and the assumption that the IRA is effective at the start of 2022, whereas the law took effect in 2022Q3; real-world construction and supply-chain frictions can also delay the observed response.

5 The IRA's Emissions and Welfare Effects

The IRA's two instruments operate through opposing channels in an open economy. The energy subsidy reinforces the existing global specialization. By stimulating domestic demand that is met by imports from incumbent low-cost producers, it allows the global economy to continue benefiting from efficient production patterns. In contrast, the equipment subsidy seeks to disrupt this specialization by shifting production to the U.S.. This move slows productivity growth in today's efficient exporting countries by denying them scale and learning-by-doing, thereby distorting global produc-

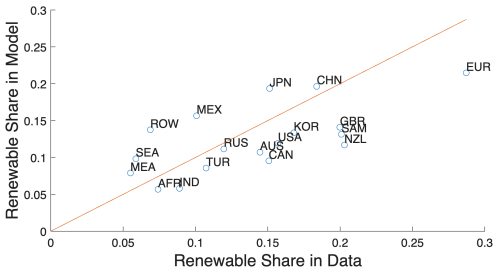
[25] Cross-border electricity trade is common within the interconnected EU market. In the quantification, I aggregate EU member states into a single region, so those intra-EU flows are internal to that region. The "non-tradable" assumption applies to electricity across model regions (e.g., EU vs. U.S.), not within the aggregated EU market.

[26] Because OECD-IO does not separately identify renewable energy sectors, I use Energy Institute (2024) via Our World in Data to measure the fossil vs. renewable split in primary energy.

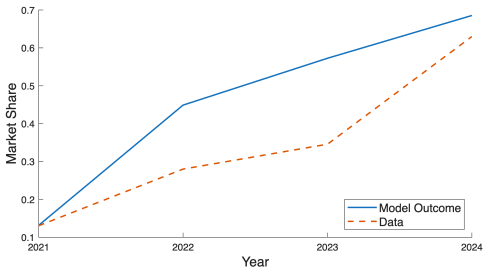
[27] Since only the capacity is observed, I apply a 71% module utilization rate from InfoLink Consulting (2023).

Figure 2: Model Validation

(a) Renewable Energy Share: Model vs. Data (2021)



(b) U.S. Domestic Solar Equipment Share, $\pi^{S}_{US,US}$



Notes: Panel (a) plots renewable shares in the data (x-axis) against model outcomes (y-axis); the 45-degree line is shown. Panel (b) plots the model (solid blue) and an empirical series (red dashed) for U.S. domestic solar equipment share from 2021 to 2024 (see footnote for data assumptions).

Table 5: Model Validation

Moment	**Model**	**Data**
(a) Matched moments		
China share in global solar equipment production	82%	82%
China share in global wind equipment production	65%	65%
Global renewable share in primary energy	15%	15%
(b) Non-targeted moments		
Equipment share in global GDP (2021)	0.16%	0.12%
Initial renewable share by country (2021)	See Fig. 2 Panel (a)	
U.S. domestic solar equipment share under IRA	See Fig. 2 Panel (b)	

tion and reducing the gains from trade. The following quantitative analysis reveals a central tension arising from this trade-off: green industrial policies that generate national economic gains for the U.S. often do so at the expense of global economic welfare, and vice-versa.

This section measures how the IRA's energy and equipment subsidies operate—separately and jointly—through prices, learning, emissions, and welfare. We first map the policy scenarios to model objects and the welfare decomposition, then isolate the role of equipment trade in shaping incidence.

Policy experiments and scenarios. I consider four scenarios relative to the no-policy baseline: (i) the full IRA (both energy and equipment subsidies), (ii) energy subsidy only, (iii) equipment subsidy only, and (iv) the full IRA with equipment trade shut down (to isolate the role of international equipment markets).

Mapping policy to model. The IRA combines a production-side tax credit for renewable electricity and a manufacturing credit for equipment (Section 45X). I implement the IRA as ad-valorem subsidy rates: 20 percent for renewable-energy production and 30 percent for equipment manufacturing.

- Energy subsidy (20 percent ad-valorem). The 2022 PTC of \$0.0275/kWh, relative to the av-

erage US retail electricity price of \$0.1236/kWh (EIA, 2023), implies a 20% output-price subsidy to renewable energy.[28]

- Equipment subsidy (30 percent ad-valorem). The 45X schedule totals about \$0.14/W for a standard solar module (polysilicon, wafer, cell, and module). With a 2022 domestic module price of roughly \$0.44/W, this yields a 30% ad-valorem equivalent for solar equipment. Wind components are likewise eligible under 45X; mapping per-unit credits to 2022 U.S. cost shares yields an ad-valorem rate of approximately 30% rate.
- Phaseout. In years 2029–2031 the subsidy rates decline to 75%, 50%, and 25% of their initial levels, respectively.

Welfare decomposition and fiscal cost. I evaluate welfare using the function defined in (1), replacing the infinite horizon with a finite sum through 2100 focusing on the transition rather than very long–run steady states.[29] Changes in welfare in country n can be decomposed as:

$$d\ln W_n = \underbrace{d\ln\left(\frac{E_n}{P_n}\right)}_{\Delta\text{real income}} - \underbrace{d\ln(1+SCC_t(Z_t-Z_0))}_{\Delta\text{carbon disutility}}, \tag{25}$$

where the first term captures movements in real income (including general-equilibrium price and factor-income effects and the fiscal cost of subsidies) and the second term captures the change in disutility from cumulative emissions. Under the calibration, total IRA outlays over 2022–2031 are approximately \$243bn: about \$118bn for the energy subsidy and \$125bn for the equipment subsidy.[30]

Role of equipment trade. Scenario (iv) sets equipment trade costs to infinity (for $k \in \{S, W\}$), holding other policies fixed. This counterfactual removes two key channels: (i) international price pass-through—foreign buyers no longer benefit from lower US equipment prices—and (ii) cross-border effect of learning-by-doing—domestic cumulative output does not expand via export demand, muting future cost declines at home and abroad. Comparing (i) and (iv) therefore isolates the contribution of equipment-market integration to the IRA's effects on prices, emissions, and welfare.

5.1 Effects on Production Geography and Prices

U.S. Production Share in Global Renewable-Equipment Supply. Figure 3 plots the U.S. production share in global renewable energy equipment from 2021 to 2050: baseline (blue solid), IRA (red dashed), and the IRA's components—energy (yellow circles) and equipment (purple dotted). The two instruments operate on different margins—one on domestic energy demand, the other on domestic equipment supply—so they shape the geography of production and prices in distinct ways.

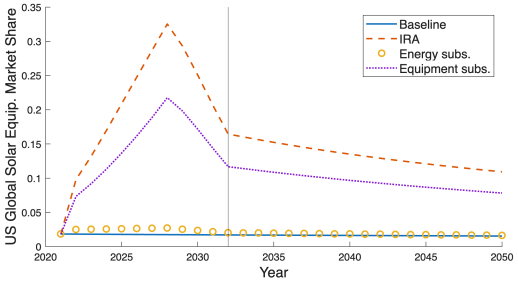
[28] Producers can elect Production Tax Credit (PTC) or Investment Tax Credit (ITC); for consistency with the model's flow-based energy production, I treat the PTC as the operative instrument. Appendix B.1 details the mapping.

[29] I measure welfare changes using consumption-equivalent variation (CEV); see Appendix A.3 for the derivation.

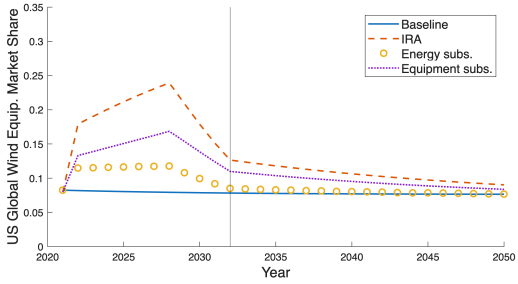
[30] See Appendix C.2 for a detailed discussion of the fiscal cost, including comparisons with estimates in the literature.

Figure 3: U.S. Production Share in Global Renewable-Equipment Supply

(a) Solar Equipment



(b) Wind Equipment



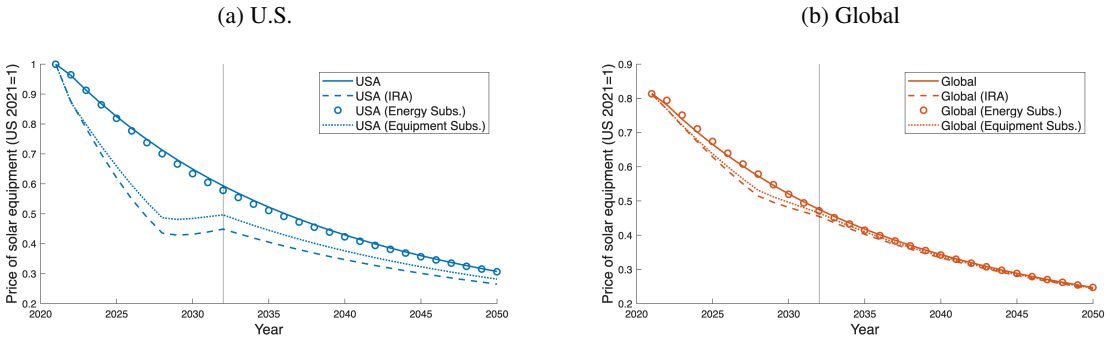
Note: This figure shows the evolution of the U.S. share of the global equipment market. Panel (a) illustrates the solar equipment market share. The solid blue line represents the share under the baseline scenario, while the red dashed line shows the share under the full IRA subsidy. The yellow circles represent the share when only the energy subsidy in the IRA is implemented, and the purple dotted line shows the share when only the equipment subsidy is implemented. Panel (b) presents the evolution of the U.S. production share in global wind equipment market under each scenario.

An *energy subsidy* stimulates domestic renewable demand and raises derived demand for equipment, but because equipment is tradable, most of that extra demand is satisfied by imports from established low-cost suppliers. Consistent with this mechanism, the energy-only case (yellow circles) lifts the U.S. solar-equipment share by only about 2.7 percentage points at its peak. The same demand push puts mild upward pressure on the global equipment price index, which can slow other countries' transitions (carbon leakage). Circles in Panels (a)–(b) of Figure 4 show this modest price effect in the U.S. and globally.

By contrast, an *equipment subsidy* directly reduces U.S. production costs, shifts comparative advantage, and displaces foreign suppliers in both domestic and export markets. The equipment-only case (purple dotted) increases the U.S. global solar-equipment share by roughly 21.2 percentage points at the peak. Scale and learning-by-doing amplify these gains, and the larger global supply lowers the world equipment price index, making the transition cheaper abroad (dotted lines in Figure 4).

The full IRA combines these channels: the equipment subsidy first expands domestic equipment production so that the subsequent demand surge from the energy subsidy is met by U.S. producers. This interaction intensifies learning-by-doing more than either policy alone, pushes the U.S. solar-equipment share to a peak of about 32.1%, and yields larger effects on equipment prices both domestically and globally (dashed lines in Figure 4). The effect is smaller for wind equipment, where initial U.S. market share is higher. After the subsidies expire in 2031, learning-induced productivity gains keep the U.S. share above the baseline for a time, but the advantage gradually erodes and the share returns toward its initial level—indicating that the policy's effects are ultimately transitory.

Figure 4: Price of Solar Energy Equipment



Notes: Evolution of solar-equipment prices, 2021–2050. Panel (a) shows the U.S.; panel (b) shows the global (installation-weighted) index. Lines denote baseline (solid), IRA (dashed), energy subsidy (circles), and equipment subsidy (dotted). Wind-equipment price levels (index) are reported in Appendix Figure C.1.

5.2 Global Spillovers: Carbon Emissions, Real Income Effect, and Welfare

This section quantifies how the IRA's two instruments affect the welfare in the United States and, in turn, propagate internationally through prices, trade in renewable equipment, and learning-by-doing.

Global Carbon Outcomes. I first focus on the aggregate global CO_2 reductions achieved by each subsidy, while the quantitative outcome of cross-country incidence—who abates where—is deferred to the appendix Section C.3. The first column of Table 6 summarizes aggregate CO_2 reduction effect. The energy subsidy lowers global CO_2 by 0.16%, primarily through abatement in the U.S. The equipment subsidy delivers a larger aggregate cut of 0.27% by pushing down global equipment prices, spreading abatement across countries. Given comparable fiscal magnitudes ($117bn vs. $125bn), the equipment subsidy is roughly 1.6 times more effective per dollar at reducing global CO_2. Combining both channels, the IRA achieves the largest reduction, 0.63% by 2100.

Now, I decompose total welfare into its real-income and carbon components, following equation (25), for each instrument (energy, equipment) and for the combined IRA. "Global" aggregates are working-age-population-weighted across countries (including the U.S.). Aggregate total welfare outcomes are in Table 6; cross-country heterogeneity is visualized in Figure 5, which plots, for each country, the impact under the energy subsidy on the horizontal axis and under the equipment subsidy on the vertical axis. Country groups are indicated by colors (net equipment exporters, net equipment importers, and fossil-fuel exporters); group averages are reported in Appendix Table C.1, and country-level values appear in Table C.2.

Real-income Effects. Reading Figure 5 Panel (a) left to right and bottom to top, the U.S. lies in the second quadrant: the energy subsidy lowers U.S. real income (import pass-through), while the equipment subsidy raises it (domestic cost declines and learning). Net equipment exporters (brown dots) are typically worse off under the equipment subsidy but better off under the energy subsidy, placing them in the fourth quadrant. By contrast, net equipment importers (green dots) cluster in the

Table 6: Welfare and CO_2 Outcomes by Instrument — Baseline Model

	Global CO_2 (%)	Global Welfare (%)	U.S. Welfare (%)
Energy subsidy	-0.16	0.03	-0.04
Equipment subsidy	-0.27	-0.00	0.08
IRA	-0.63	0.03	0.05

Notes: Reported values are cumulative through 2100. Global welfare is a working-age-population–weighted aggregate across countries (including the U.S.), using baseline-year shares.

first quadrant and above the 45° line, indicating they gain under both instruments and gain more from the equipment subsidy than from the energy subsidy. Finally, fossil-fuel exporters tend to occupy the third quadrant, losing real income under both policies as global fossil demand weakens.[31] In aggregate real-income terms, the equipment subsidy is globally negative (-0.03%), whereas the energy subsidy is globally neutral (0.00%).

Total Welfare: Adding the Carbon Benefit. Figure 5 Panel (b) adds the climate component to the real-income effects, moving points northeast overall. Quantitatively, the carbon channel adds 0.03 percentage points to welfare under both the energy subsidy (shifting dots right) and the equipment subsidy (shifting dots up), so total welfare reflects both terms-of-trade/learning and discounted emissions gains.[32] Aggregates in Table 6 make the trade-off clear: the energy subsidy benefits the global economy at the cost of the U.S. (global welfare 0.03%, U.S. welfare -0.04%), whereas the equipment subsidy benefits the U.S. more (U.S. welfare 0.08% vs. global welfare $\approx 0\%$).

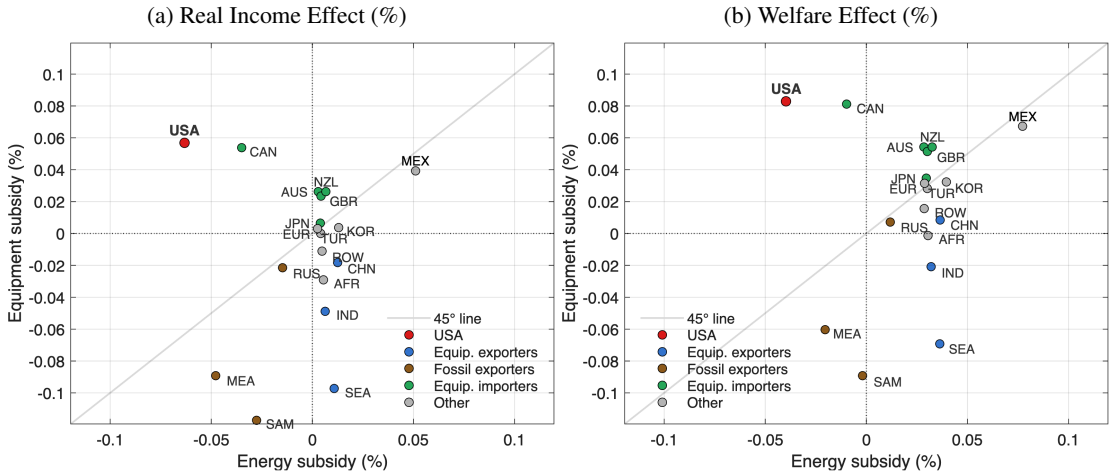
Combined Policy (IRA). Table 6 reports the headline effects: global CO_2 falls by 0.63% by 2100, while total welfare rises for both the world $(+0.03\%)$ and the United States $(+0.05\%)$. The subsidies are complementary: the equipment subsidy expands domestic supply so that the demand surge from the energy subsidy is absorbed at home, amplifying U.S. learning-by-doing rather than leaking to imports.

Figure 6 unpacks the distributional channels behind these aggregates. Panel (a), in the open-economy baseline, shows that the real-income component of the IRA is slightly negative for the U.S. (-0.01%), reflecting that the energy component is relatively costly. Distributionally, incumbent equipment exporters (SEA, IND, CHN) face adverse terms of trade and reduced scale, and fossil-fuel exporters (MEA, SAM, RUS) are hit by lower fossil demand. Many net equipment importers register small real-income gains from cheaper equipment, but these are not large enough to offset the

[31] Canada and Mexico are informative exceptions. Canada exports fossil fuels but also supplies intermediates for U.S. equipment production; Mexico is a net fossil-fuel importer from the U.S. and imports U.S. equipment. Both countries benefit more from the equipment subsidy (via U.S. manufacturing expansion and trade), but the energy subsidy has different implications across them due to their distinct fossil and intermediate trade positions.

[32] One might expect a strictly larger carbon benefit for the equipment subsidy because it reduces more CO_2 by 2100. The similarity in welfare magnitudes arises from timing: energy support induces immediate abatement during the policy window, while equipment support works through investment and diffusion, with more of its abatement arriving later. With discounting that values earlier abatement more, the present-value carbon benefits are similar across the two instruments.

Figure 5: Real Income and Total Welfare Effect of Subsidies



Notes: Each panel plots percent changes relative to the baseline, aggregated (discounted) to 2100 by country, with country groups distinguished by colors. Each point is a country. The horizontal axis reports the impact under the energy subsidy; the vertical axis reports the impact under the equipment subsidy. Panel (a) shows the real-income component (excluding carbon damages). Panel (b) shows total welfare, which adds the carbon benefit to real income.

global aggregate loss (about -0.04%). The equipment component reorients production away from high-learning incumbents, weakening global specialization; as a result, global gains from trade fall, and in pure real-income terms the IRA is difficult to justify absent its carbon benefit. Panel (b) adds the carbon component and shifts the distribution upward, making total welfare positive for both the U.S. and the global aggregate despite the real-income loss.

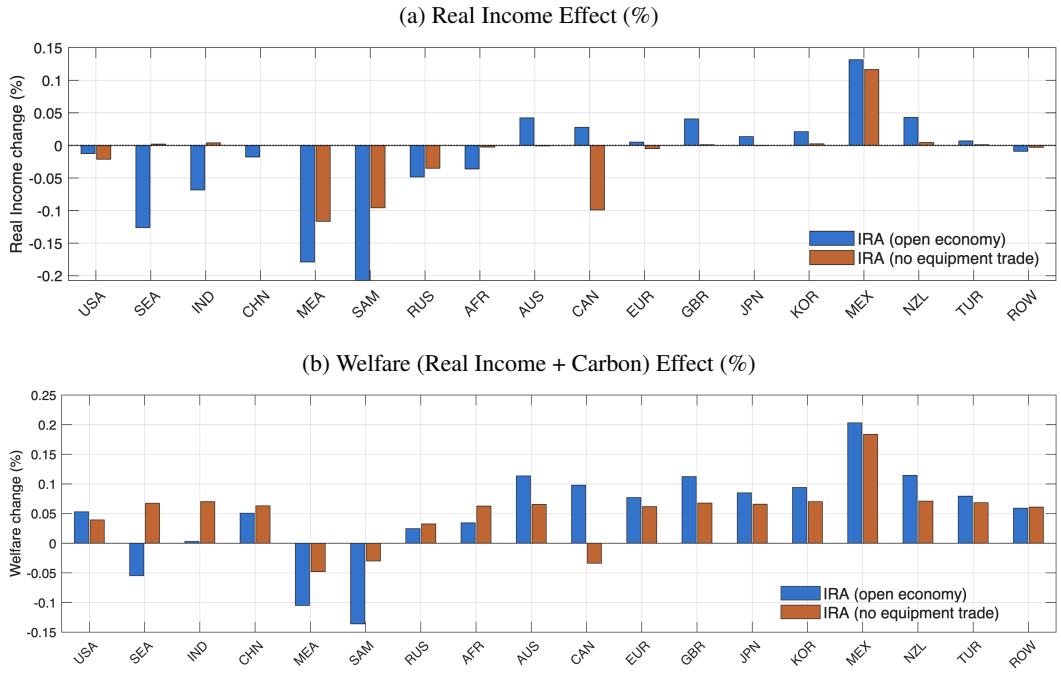
Optimal Subsidy. A natural question is which subsidy mix is optimal from a unilateral U.S. perspective. While deriving closed-form solutions is beyond the scope of this paper, I evaluate welfare and carbon outcomes on a grid of energy–equipment subsidy pairs. Figure C.3 displays U.S. and global welfare across the subsidy space; a full characterization is provided in Appendix Section C.5.

From the U.S. perspective, the IRA mix is not optimal: the U.S.-optimal policy features no energy subsidy and a 40 percent equipment subsidy rate because demand-side aid mostly bids up imported equipment and transfers gains to foreign equipment suppliers, whereas a production-side subsidy amplifies domestic learning-by-doing and persistent cost declines, and thus provides both real income gains and further decarbonization that benefits the U.S. welfare. Relative to the IRA, this policy further reduces the global CO_2 and substantially raises U.S. welfare, while leaving global welfare essentially flat: global CO_2 falls by 0.79%, global welfare change is 0.00%, and U.S. welfare rises by 0.14%.

Robustness. Here I highlight two robustness checks—one on the demand side (renewable–fossil substitutability) and one on the supply side (global LBD spillovers).

(i) Higher substitutability ($\psi = 5$): Both instruments deliver larger reductions in CO_2 emissions, but the welfare ranking is unchanged: the equipment-manufacturing subsidy reduces global CO_2

Figure 6: Real Income and Welfare Effects of the IRA (with and without Equipment Trade)



Note: This Figure plots the impact of the IRA under the baseline model and the alternative model without equipment trade. Panel (a) shows the real-income component (excluding carbon damages) of the welfare effect of IRA. Panel (b) shows total welfare, which adds the carbon benefit to real income.

more than the energy-production subsidy, while the latter yields larger global welfare gains; the equipment subsidy still raises U.S. welfare and lowers others' welfare via terms-of-trade effects.

(ii) Global LBD spillovers: Following Arkolakis and Walsh (2023), allowing frictionless cross-country LBD spillovers reduces U.S. welfare gains from the equipment subsidy as the subsidy passes through to foreign equipment producers via learning spillover, and widens the energy subsidy's global welfare gains. Despite these spillover gains, I find the IRA's energy subsidy still reduces U.S. welfare by worsening the terms of trade. This contrasts with Arkolakis and Walsh (2023), who abstract from equipment trade and find U.S. gains from the energy subsidy.

The full set of robustness analyses—including these two checks, extended policy horizons, stronger learning-by-doing, lower trade elasticities, and a heterogeneous damage function—is reported in Appendix C.10, Table C.4.

5.3 The Role of Equipment Trade

The preceding analysis demonstrates that equipment trade is a central mechanism for the IRA's global spillovers. To quantify its importance, I simulate the IRA in a counterfactual world without equip-

Table 7: Impact of the IRA with and without Equipment Trade

	Global CO_2 (%)	Global welfare (%)	U.S. welfare (%)
Baseline (with equipment trade)	−0.63	0.03	0.05
No equipment trade	−0.42	0.06	0.04

ment trade and compare the results to the baseline, as shown in Table 7.[33]

Abstracting from equipment trade fundamentally alters the policy's perceived impact. An analysis without trade would underestimate the IRA's climate effectiveness, predicting a smaller global emissions cut (−0.42% vs. −0.63% with trade). It would also overestimate the global welfare gain (0.06% vs. 0.03%) and underestimate the U.S. welfare gain (0.04% vs. 0.05%). The differing effects of the IRA's individual energy and equipment subsidy components in this counterfactual are detailed in Appendix C.6.

The heterogeneous incidence across countries, visible in Figure 6, reveals why these aggregate effects change. With equipment trade (blue bars), the IRA delivers broader emissions cuts across countries because lower U.S. equipment costs are passed on internationally, accelerating the foreign energy transition. Without this trade channel (red bars), many non-U.S. countries see higher emissions, reflecting the loss of this international diffusion. In economic aspect, the reason is that the beggar-thy-neighbor channel of the IRA, in particular the equipment subsidy component, disappears: foreign producers are no longer displaced from equipment markets, so productivity gains abroad (e.g., in China, India, and Southeast Asia) are not suppressed. As a result, welfare effects also shift: equipment exporters see additional gains while equipment importers no longer benefit from cheaper U.S. goods, and fossil fuel exporters loss less due to slower energy transition. The gains, mostly coming from carbon emissions reduction, become more even across countries.

6 Extensions

In this section, I extend the counterfactual analysis along two dimensions. First, I pair the IRA with a trade policy that raises U.S. tariffs on imported solar equipment. Second, I allow for policy responses by other major economies (China and the EU). For comparability, all outcomes are summarized in Table 8.

[33] Here I focus on how trade mediates the *impacts* of the IRA. How trade shapes the *speed* of the transition is covered in Appendix Section C.7.1; I also study the role of learning-by-doing in Appendix Section C.7.2.

6.1 Impact of the IRA under Trade Policy

Setup. I impose a 50% ad valorem tariff on solar equipment imported from China and Southeast Asia into the U.S. for 2022–2031 (hereafter, the *solar tariff*), mirroring recent U.S. policy.[34] The model with tariffs is described in Appendix A.4.

Trade policy in isolation. Absent industrial policy, higher trade barriers can partially correct misallocation from localized learning-by-doing by redirecting demand toward domestic production. However, consistent with Lashkaripour and Lugovskyy (2023), this is a blunt tool: the tariff raises delivered equipment prices, slows installation, and delays decarbonization. In Table 8 (panel (b), row "Tariff"), global CO_2 rises by 0.01% and both global and U.S. welfare fall (-0.01% and -0.02%, respectively).

Combining the tariff with the IRA. Pairing the tariff with the IRA's subsidies protects the home market while lowering domestic marginal costs, modestly strengthening U.S. penetration in solar equipment relative to IRA alone. As shown in Table 8 (panel (b), row "IRA + Tariff"), global CO_2 falls by *about* 0.63% (very similar to the baseline IRA), while global and U.S. welfare remain essentially unchanged at 0.03% and 0.05%, respectively. This suggests the tariff's static distortions are largely offset by the IRA subsidies, with learning-by-doing amplifying domestic penetration even though aggregate welfare effects are similar.

6.2 U.S.–China–EU Policy Competition

Setup. I allow China and the EU to implement the same IRA-style subsidies as the U.S.—separately by instrument (energy only, equipment only) and in combination (IRA). Although this is not a full strategic model, it is informative about coordination and leakage when major blocs act together. The quantitative results are reported in Table 8; below we summarize each case. Country-level incidences are discussed in Appendix Section C.9.

Energy subsidy (U.S.–China–EU). Multilateral energy subsidies reduce global CO_2 by 0.85% and raise global welfare by 0.07%, while U.S. welfare increases by a smaller 0.04% (Table 8, panel (c)). The gap (global $>$ U.S.) reflects the U.S. position as a net *importer* of renewable equipment: when all blocs stimulate renewable demand, terms-of-trade and scale gains accrue relatively more to equipment producing countries (notably China and the EU). Compared to the case when only the U.S. implement energy subsidy, the U.S. now records a positive welfare gain as partner economies decarbonize domestically and carbon leakage falls.

Equipment subsidy (U.S.–China–EU). When all three subsidize equipment production, global CO_2 falls by 1.81% and global welfare rises by 0.10%, while the U.S. enjoys a much larger welfare gain of 0.30%. When all three blocs subsidize, U.S. equipment's global share is mechanically smaller

[34] In 2024 the U.S. announced higher Section 301 tariffs on Chinese solar cells (up to 50%). Several Chinese-affiliated manufacturers located in Southeast Asia account for a large share of U.S. solar imports and have faced preliminary duties.

than in the "U.S.-only" case due to intensified competition.[35] Even with intensified competition, the U.S. gains disproportionately because the U.S. - as a net equipment importer - benefits significantly from importing cheaper, subsidized solar and wind equipment from China and EU, respectively. This improves its terms of trade, accelerates the energy transition, and boosts domestic welfare.

Full IRA (U.S.–China–EU). Combining both instruments delivers the largest overall effects: global CO_2 decreases by 2.97%, global welfare rises by 0.14%, and U.S. welfare increases by 0.33%. The energy component drives broad deployment (reducing leakage when major economies participate), while the equipment component diffuses cost reductions internationally and sustains dynamic productivity gains.

Table 8: Equilibrium Comparison

	Global CO_2 (%)	Global Welfare (%)	U.S. Welfare (%)
(a) Baseline specification			
IRA	-0.63	0.03	0.05
(b) IRA + Solar Tariff			
Tariff (10yr)	0.02	-0.01	-0.02
Energy Subs. + Tariff	-0.15	0.02	-0.04
Equipment Subs. + Tariff	-0.28	0.00	0.08
IRA + Tariff	-0.66	0.03	0.05
(c) U.S.–China–EU Policy			
Energy Subs.	-0.85	0.07	0.04
Equipment Subs.	-1.81	0.10	0.30
IRA	-2.97	0.14	0.33

7 Conclusion

The transition to renewable energy relies heavily on the trade of renewable energy equipment, such as solar panels and wind turbines. Motivated by this, this paper develops a multi-country dynamic general-equilibrium trade model in which renewable-energy equipment is tradable and learning-by-doing is local to equipment manufacturing. Applied to the IRA, allowing for equipment trade changes both the distribution of gains and the cost path: global CO_2 falls by 0.63% and welfare rises for the U.S. (0.05%) and globally (0.03%), with part of the environmental benefit operating through accelerated adoption abroad. Abstracting from equipment trade would lead one to conclude that the IRA benefits the global economy more than the U.S. (global 0.06% vs. U.S. 0.04%), underscoring that policy evaluation must account for equipment tradability and the geographic locus of learning.

Comparing policy instruments highlights distinct roles. Equipment subsidy component in the IRA, compared to energy subsidy component, benefits U.S. welfare at the expense of global welfare,

[35] See Appendix Section C.9 for further details.

while energy subsidies work in the opposite way. Additionally, while energy subsidies are more effective at reducing US carbon emissions, equipment subsidies have a greater global carbon reduction impact by facilitating the energy transition in other countries through lowering the global cost of equipment.

References

Acemoglu, Daron, Philippe Aghion, Leonardo Bursztyn, and David Hemous, "The Environment and Directed Technical Change," *American Economic Reivew*, February 2012, *102* (1), 131–166.

_ , Ufuk Akcigit, Douglas Hanley, and William Kerr, "The Transition to Clean Technology," *Journal of Political Economy*, 2016, *124* (1), 52–104.

Aldy, Joseph E., Todd D. Gerarden, and Richard L. Sweeney, "Investment versus Output Subsidies: Implications of Alternative Incentives for Wind Energy," *Journal of the Association of Environmental and Resource Economics*, 2023, *10* (4), 981–1018.

Alvarez, Fernando and Robert E. Jr. Lucas, "General equilibrium analysis of the Eaton–Kortum model of international trade," *Journal of Monetary Economics*, September 2007, *54* (6), 1726–1768.

Arkolakis, Costas and Conor Walsh, "Clean Growth," *Working Paper*, 2023.

Baker, Erin, Meredith Fowlie, Derek Lemoine, and Stanley S. Reynolds, "The Economics of Solar Electricity," *Annual Review of Resource Economics*, 2013, *5*, 387–426.

Baldwin, Robert E., "The Case against Infant Industry Protection," *Journal of Political Economy*, 1969, *77* (3), 295–305.

Banares-Sanchez, Ignacio, Robin Burgess, David Laszlo, Pol Simpson, John Van Reenen, and Yifan Wang, "Chinese Innovation, Green Industrial Policy and the Rise of Solar Energy," *Working Paper*, 2024.

Bardhan, Pranab K., "On Optimum Subsidy to a Learning Industry: An Aspect of the Theory of Infant-Industry Protection," *International Economic Review*, 1971, *12* (1), 54–70.

Bartelme, Dominick, Arnaud Costinot, Dave Donaldson, and Andres Rodriguez-Clare, "The Textbook Case for Industrial Policy: Theory Meets Data," *Working Paper*, 2024.

Bistline, John, Neil Mehrotra, and Catherine Wolfram, "Economic Implications of the Climate Provisions of the Inflation Reduction Act," *NBER Working Paper 31267*, 2023.

Boehm, Christoph E., Andrei A. Levchenko, and Nitya Pandalai-Nayar, "The Long and Short (Run) of Trade Elasticities," *American Economic Review*, April 2023, *113* (4), 861–905.

Bolinger, Mark, Ryan Wiser, and Eric O'Shaughnessy, "Levelized cost-based learning analysis of utility-scale wind and solar in the United States," *iScience*, 2022, *25* (6).

Bollinger, Bryan, Kenneth Gillingham, Drew Vollmer, and Daniel Xu, "Strategic Avoidance and the Welfare Impacts of Solar Panel Tariffs," *Working Paper*, 2024.

Caliendo, Lorenzo and Fernando Parro, "Estimates of the Trade and Welfare Effects of NAFTA," *The Review of Economic Studies*, 2015, *82* (1), 1–44.

_ , Marcelo Dolabella, Mauricio Moreira, Matthew Murillo, and Fernando Parro, "Voluntary Emission Restraints in Developing Economies: The Role of Trade Policy," *Working Paper*, 2024.

Casey, Gregory, Woongchan Jeon, and Christian Traeger, "The Macroeconomics of Clean Energy

Subsidies," *Working Paper*, 2023.

Choi, Jaedo and Andrei A. Levchenko, "The Long-Term Effects of Industrial Policy," *Journal of Monetary Economics*, June 2025, *152*, 103779.

Congressional Budget Office, "The Budget and Economic Outlook: 2024 to 2034," 2024.

Covert, Thomas R. and Richard L. Sweeney, "Winds of Change: Estimating Learning by Doing without Cost or Input Data," *Working Paper*, 2024.

Cruz, José-Luis and Esteban Rossi-Hansberg, "The Economic Geography of Global Warming," *The Review of Economic Studies*, March 2024, *91* (2), 899–939.

Donald, Eric, "Spillovers and the Direction of Innovation," *Working Paper*, 2024.

Eaton, Jonathan and Samuel Kortum, "Technology, Geography, and Trade," *Econometrica*, 2002, *70* (5), 1741–1779.

_ , _ , Brent Neiman, and John Romalis, "Trade and the Global Recession," *American Economic Reivew*, 2016, *106* (11), 3401–3438.

EIA, "State Electricity Profiles," 2023, *https://www.eia.gov/electricity/state/unitedstates/.*

Energy Institute, "Statistical Review of World Energy," 2024.

EPA, "Report on the Social Cost of Greenhouse Gases: Estimates Incorporating Recent Scientific Advances," 2023.

Ethier, Wilfred J., "National and International Returns to Scale in the Modern Theory of International Trade," *American Economic Review*, 1982, *72* (3), 389–405.

Farrokhi, Farid and Ahmad Lashkaripour, "Can Trade Policy Mitigate Climate Change?," *Working Paper*, 2024.

Fontagné, Lionel, Houssein Guimbard, and Gianluca Orefice, "Tariff-based product-level trade elasticities," *Journal of International Economic*, 2022, *137*, 103593.

Garcia-Lembergman, Ezequiel Natalia Ramondo, Andres Rodriguez-Clare, and Joseph S. Shapiro, "The Carbon Footprint of Multinational Production," *Working Paper*, 2023.

Gentile, Claudia, "Relying on Intermittency: Clean Energy, Storage, and Innovation in a Macro Climate Model," *Working Paper*, 2024.

Gerarden, Todd, "Demanding Innovation: The Impact of Consumer Subsidies on Solar Panel Production Costs," *Management Science*, 2023, *69* (12), 7151–7882.

Global Wind Energy Council, "Mission Critical: Building the Global Wind Energy Supply Chain for a 1.5C World," 2023.

Goldberg, Pinelopi K., Réka Juhász, Nathan J. Lane, Giulia Lo Forte, and Jeff Thurk, "Industrial Policy in the Global Semiconductor Sector," *NBER Working Paper*, 2024, *32651.*

Greenwood, Jeremy, Zvi Hercowitz, and Per Krusell, "Long-Run Implications of Investment-Specific Technological Change," *American Economic Review*, 1997, *87* (3), 342–362.

Groote, Olivier De and Frank Verboven, "Subsidies and Time Discounting in New Technology Adoption: Evidence from Solar Photovoltaic Systems," *American Economic Review*, 2019, *109* (6),

2137–2172.

Gugler, Klaus, Adhurim Haxhimus, and Mario Liebensteiner, "Effectiveness of climate policies: Carbon pricing vs. subsidizing renewables," *Journal of Environmental Economics and Management*, 2021, *106*, 102405.

Head, Keith and John Ries, "Increasing Returns versus National Product Differentiation as an Explanation for the Pattern of U.S.-Canada Trade," *American Economic Reivew*, September 2001, *91* (4), 858–876.

Hitaj, Claudia and Andreas Löschel, "The impact of a feed-in tariff on wind power development in Germany," *Resource and Energy Economics*, 2019, *57*, 18–35.

Hsiao, Allan, "Coordination and Commitment in International Climate Action: Evidence from Palm Oil," *Working Paper*, 2024.

InfoLink Consulting, "Supply Chain Utilization Rate Report," July 2023.

Jo, Ara, "Substitution between Clean and Dirty Energy with Biased Technical Change," *Working Paper*, 2023.

Ju, Jiandong, Hong Ma, Zi Wang, and Xiaodong Zhu, "Trade wars and industrial policy competitions: Understanding the US-China economic conflicts," *Journal of Monetary Economics*, 2024, *141*, 42–58.

Kortum, Samuel E. and David A. Weisbach, "Optimal Unilateral Carbon Policy," *Working Paper*, 2021.

Krugman, Paul, "The Narrow Moving Band, the Dutch Disease, and the Competitive Consequences of Mrs. Thatcher," *Journal of Development Economics*, 1987, *27*, 41–55.

Lashkaripour, Ahmad and Volodymyr Lugovskyy, "Profits, Scale Economies, and the Gains from Trade and Industrial Policy," *American Economic Review*, 2023, *113* (10), 2759–2808.

Oakleaf, James R., Christina M. Kennedy, Sharon Baruch-Mordo, James S. Gerber, Paul C. West, Justin A . Johnson, and Joseph Kiesecker, "Mapping global development potential for renewable energy, fossil fuels, mining and agriculture sectors," *Scientific Data*, 2019, *6* (101).

Papageorgiou, Chris, Marianne Saam, and Patrick Schulte, "Substitution Between Clean And Dirty Energy Inputs," *The Review of Economics and Statistics*, May 2017, *99* (2), 281–290.

Parro, Fernando, "Capital-Skill Complementarity and the Skill Premium in a Quantitative Model of Trade," *American Economic Journal: Macroeconomics*, 2013, *5* (2), 72–117.

Penn Wharton Budget Model, "Update: Budgetary Cost of Climate and energy provisions in the Inflation Reduction Act," 2023.

Ravikumar, B., Ana Maria Santacreu, and Michael Sposi, "Capital accumulation and dynamic gains from trade," *Journal of International Economics*, 2019, *119*, 93–110.

Ricke, Katharine, Laurent Drouet, Ken Caldeira, and Massimo Tavoni, "Country-level social cost of carbon," *Nature Climate Change*, 2018, *8*, 895–900.

Shapiro, Joseph S., "The Environmental Bias of Trade Policy," *The Quarterly Journal of Economics*,

2021, *136* (2), 831–886.

Shin, David D., "Climate Policies under Dynamic Factor Adjustment," *Working Paper*, 2024.

U.S. Department of Energy, "Land-Based Wind Market Report: 2023 Edition," 2023.

Wiskich, Anthony, "Perfect So Far? Substitutability Between Wind & Solar and Dirty Electricity Generation," *Working Paper*, 2023.

Wood Mackenzie, "Market Report US Solar Market Insight: Q2 2024," June 2024.

Xiang, Wei, "Clean Growth and Environmental Policies in the Global Economy," *Working Paper*, 2023.

Appendix: Green Industrial Policy in a Globalized Economy

Sungwan Hong
University of Pittsburgh

Appendix A Derivations **1**
A.1 Composite Intermediate Goods (Dixit–Stiglitz) 1
A.2 Deriving Share of Each Energy Source in Production and Consumption 1
A.3 Measuring Welfare: Consumption Equivalent Variation 2
A.4 A Model with Tariff 2

Appendix B Calibration: Data and Estimation **3**
B.1 Renewable Energy Provisions in the IRA 3
B.2 Geographic and Time Coverage 4
B.3 Data for Section 2.1 5
B.4 Data Construction in LBD Estimation (Section 4.4) 6
B.5 Renewable Potential 7
B.6 Measuring Initial Capital Stocks 10
B.7 Calibrating the Damage Parameter 11

Appendix C Additional Results **12**
C.1 Impact of Subsidies on Wind Equipment Price 12
C.2 Estimated Fiscal Cost and Instrument Complementarities 13
C.3 Who Reduces Carbon Emissions? 13
C.4 Welfare Decomposition 13
C.5 Optimal Subsidy 15
C.6 The Role of Equipment Trade for Individual Subsidies 16
C.7 Comparative Statics 18
C.8 Additional Results on IRA under Trade Policy 19
C.9 Additional Results on U.S.-China-EU Policy Competition 20
C.10 Robustness Check 22

Appendix D Algorithm **25**

Appendix A Derivations

A.1 Composite Intermediate Goods (Dixit–Stiglitz)

Composite producers in sector j aggregate a unit continuum of varieties $\omega^j \in [0,1]$ via

$$Q^j_{n,t} = \left[\int_0^1 f^j_{n,t}(\omega^j)^{\frac{\sigma^j-1}{\sigma^j}} \, d\omega^j \right]^{\frac{\sigma^j}{\sigma^j-1}},$$

where $\sigma^j > 1$ is the elasticity across varieties. Cost minimization yields variety demand

$$f^j_{n,t}(\omega^j) = \left(\frac{p^j_{n,t}(\omega^j)}{P^j_{n,t}} \right)^{-\sigma^j} Q^j_{n,t},$$

and the sectoral price index

$$P^j_{n,t} = \left[\int_0^1 p^j_{n,t}(\omega^j)^{1-\sigma^j} \, d\omega^j \right]^{\frac{1}{1-\sigma^j}}.$$

These expressions underpin the notation in the main text.

A.2 Deriving Share of Each Energy Source in Production and Consumption

Due to the Nested CES structure in energy production, the share of each energy source $e \in \{s, w, f\}$ in producing j sector good is endogenously determined.

$$\begin{aligned}
\gamma^{M,fj}_n &= [\gamma^{E,j}_n \gamma^j_n] \Big[1 + \frac{\eta_e}{1-\eta_e} \Big(\frac{p^f_n}{p^r_n} \Big)^{\psi-1} \Big]^{-1} \\
\gamma^{M,sj}_n &= [\gamma^{E,j}_n \gamma^j_n] \Big[1 + \frac{1-\eta_e}{\eta_e} \Big(\frac{p^r_n}{p^f_n} \Big)^{\psi-1} \Big]^{-1} \Big[1 + \frac{1-\eta_r}{\eta_r} \Big(\frac{p^s_n}{p^w_n} \Big)^{\rho-1} \Big]^{-1} \\
\gamma^{M,wj}_n &= [\gamma^{E,j}_n \gamma^j_n] \Big[1 + \frac{1-\eta_e}{\eta_e} \Big(\frac{p^r_n}{p^f_n} \Big)^{\psi-1} \Big]^{-1} \Big[1 + \frac{\eta_r}{1-\eta_r} \Big(\frac{p^w_n}{p^s_n} \Big)^{\rho-1} \Big]^{-1}
\end{aligned}$$

where $p^{r,j}_n y^{r,j}_n = p^s_n y^{s,j}_n + p^w_n y^{w,j}_n$ and $p^E_n y^{E,j}_n = p^f_n y^{f,j}_n + p^r_n y^{r,j}_n$

Similar formula can be derived for share of each energy source in utility:

$$
\begin{aligned}
\mu_n^f &= [\mu_n^E]\Big[1+\frac{\eta_e}{1-\eta_e}\Big(\frac{p_n^f}{p_n^r}\Big)^{\psi-1}\Big]^{-1} \\
\mu_n^s &= [\mu_n^E]\Big[1+\frac{1-\eta_e}{\eta_e}\Big(\frac{p_n^r}{p_n^f}\Big)^{\psi-1}\Big]^{-1}\Big[1+\frac{1-\eta_r}{\eta_r}\Big(\frac{p_n^s}{p_n^w}\Big)^{\rho-1}\Big]^{-1} \\
\mu_n^w &= [\mu_n^E]\Big[1+\frac{1-\eta_e}{\eta_e}\Big(\frac{p_n^r}{p_n^f}\Big)^{\psi-1}\Big]^{-1}\Big[1+\frac{\eta_r}{1-\eta_r}\Big(\frac{p_n^w}{p_n^s}\Big)^{\rho-1}\Big]^{-1}.
\end{aligned}
$$

A.3 Measuring Welfare: Consumption Equivalent Variation

Welfare in region n, W_n, is defined by the discounted sum of real income incorporating carbon emissions disutility:

$$
W_n = \sum_{s=1}^{T} \beta^{s-1}\Big(\log(E_{n,t}/P_{n,t}) + \log(1/(1+SCC(Z_t - Z_0)))\Big).
$$

To study the change in welfare under a counterfactual, I define the compensating variation in consumption for region n to be CEV_n such that

$$
W_n' = W_n + \sum_{s=1}^{T} \beta^{s-1}\log(CEV_n).
$$

where W_n' is the welfare of country n under the counterfactual. Rearranging this and taking log gives

$$
\log(CEV_n) = \frac{(W_n' - W_n)(1-\beta)}{(1-\beta^T)}.
$$

A.4 A Model with Tariff

In this section, I incorporate sectoral tariffs into the baseline model.

I consider an ad-valorem tariff, $\tau_{ni,t}^j$ that country n charges to the goods in sector j imported from country i. Now, let the total trade cost inclusive of the tariff be denoted as $d_{ni,t}^j \equiv \kappa_{ni}^j(1+\tau_{ni,t}^j)$ in equation (10). To include the tariff effect, equation (13) can be rewritten as follows:

$$
Y_{n,t}^j = \sum_{m=1}^{N} \frac{\pi_{mn,t}^j}{(1+\tau_{mn,t}^j)(1-s_{m,t}^j)} X_{m,t}^j. \tag{A.1}
$$

The equation captures that gross output in country n's sector j is equal to the sum of total exports and domestic sales, inclusive of tariffs.

To incorporate the tariff into the trade balance condition, the equation should reflect that tariffs affect the value of imports:

$$\sum_{j\in\Omega}\sum_{n=1}^{N}\frac{\pi^{j}_{in,t}}{(1+\tau^{j}_{in,t})(1-s^{j}_{i,t})}X^{j}_{i,t}-D_i=\sum_{j\in\Omega}\sum_{n=1}^{N}\frac{\pi^{j}_{ni,t}}{(1+\tau^{j}_{ni,t})(1-s^{j}_{n,t})}X^{j}_{n,t} \tag{A.2}$$

The household's total income should now include the revenue generated from tariffs:

$$\begin{aligned}
&\sum_{j\in\Omega^{*}_{K}}P^{j}_{n,t}C^{j}_{n,t}\\
&=w_{n,t}L_{n,t}+\sum_{k'\in\Omega_K}r^{k'}_{n,t}K^{k'}_{n,t}-\sum_{j\in\Omega}s^{j}_{o,t}\sum_{o=1}^{N}\frac{\pi^{j}_{on,t}}{(1-s^{j}_{n,t})}X^{j}_{o,t}+\sum_{j\in\Omega}\tau^{j}_{ni,t}X^{j}_{n,t}\sum_{i=1}^{N}\frac{\pi^{j}_{ni,t}}{(1+\tau^{j}_{ni,t})(1-s^{j}_{n,t})}\\
&+\sum_{j\in\Omega_{RE}}\Pi^{j}_{n,t}+D_n-\sum_{k\in\Omega_K}P^{k}_{n,t}I^{k}_{n,t}\\
&\equiv E_{n,t}
\end{aligned} \tag{A.3}$$

Now I can define an equilibrium with tariff.

Definition 2. ***A sequential equilibrium of the model with tariff*** *is a set of prices* $\left\{w_{n,t},P^{j}_{n,t},r^{k}_{n,t}\right\}^{N,J,K,T}_{n=1,j=1,k=1,t=1}$*, allocations of goods and labor* $\left\{\pi^{j}_{nit},l^{j}_{n,t}\right\}^{N,N,J,T}_{n=1,i=1,j=1,t=1}$ *that satisfies the static equilibrium conditions: unit costs (equations (3), (5), and (9)), trade shares ((12)), local prices (10), labor and market clearing conditions ((15),(16)), and trade balance ((A.2)), and dynamic conditions: law of motion of capitals ((18)), and Euler equation ((21)), where gross output satisfies (A.1) and household budget constraint satisfies (A.3).*

Appendix B Calibration: Data and Estimation

B.1 Renewable Energy Provisions in the IRA

In August 2022, the United States enacted the Inflation Reduction Act (IRA), the largest U.S. investment to date in clean energy and climate policy. The law provides roughly $369 billion for energy security and climate programs, including incentives for deploying renewable energy and for manufacturing clean-energy equipment (Congressional Budget Office, 2024). External analyses project that, taken together, these measures could reduce U.S. greenhouse-gas emissions to around 40% below 2005 levels by 2030.[1]

The IRA's clean-energy support operates through two main channels that map directly into the model. First, demand-side deployment incentives expand and extend the Production Tax Credit (PTC; IRC §45)—a per kWh credit for qualified generation—and the Investment Tax Credit (ITC;

[1] This is a modeled projection (e.g., from research groups and agencies), not a statutory target in the IRA.

IRC §48)—a credit for a share of project capital costs. These provisions apply to technologies including wind and solar (among others); this paper focuses on wind and solar. (For post-2024 projects, technology-neutral credits §45Y/§48E succeed the PTC/ITC, but the structure is analogous.)

Second, supply-side manufacturing incentives are delivered via the Advanced Manufacturing Production Credit (IRC §45X), which pays per-unit credits for domestic production of key components across clean-energy supply chains. For solar, covered items include PV-grade polysilicon, wafers, cells, modules, and inverters; for wind, blades, nacelles, and towers are eligible; battery cells/modules and certain critical minerals are also covered. These provisions aim to shift comparative advantage toward domestic producers by lowering marginal costs and accelerating learning-by-doing.

Where relevant, bonus credit rates tied to prevailing-wage and apprenticeship requirements, domestic content, and energy-community siting further increase effective subsidy rates, but the analysis in this paper abstracts from those compliance details and focuses on the core economic channels.

B.2 Geographic and Time Coverage

List of countries and regions. I calibrate the model to 18 countries/regions including a synthetic rest of the world. These countries/regions include Africa, Australia, Canada, China, Europe, Great Britain, India, Japan, Korea, Middle East Asia, Mexico, New Zealand, Russia, South America, South East Asia, Turkiye, United States, and the rest of the world.

Definition of the aggregated regions. The aggregated regions are defined as follows:

- Africa: Cameroon, Côte d'Ivoire, Egypt, Morocco, Nigeria, Senegal, South Africa, Tunisia
- Europe: Austria, Belgium, Bulgaria, Croatia, Cyprus, Czech, Denmark, Estonia, Finland, France, Germany, Greece, Hungary, Ireland, Italy, Latvia, Lithuania, Luxembourg, Malta, Netherlands, Norway, Poland, Portugal, Romania, Slovakia, Slovenia, Spain, Sweden, Switzerland
- Middle East Asia: Jordan, Israel, and Saudi Arabia.
- South America: Argentina, Brazil, Chile, Colombia, Costa Rica, and Peru.
- South East Asia: Bangladesh, Brunei, Cambodia, Indonesia, Laos, Malaysia, Myanmar, Philippines, Singapore, Thailand, Vietnam.

Sector aggregation. The aggregated sectors are defined in table B.1.

Time horizon. I treat 2021 as the starting point of the model and collect from various data sources the information necessary for constructing this initial economy. While the model has infinite horizon, I report some of the results focusing on the years 2021–2050. I treat each period in the model as one year.

Table B.1: Sector Aggregation

Aggregated Industry	Code in OECD-IO	Industry in OECD-IO
Agriculture and Mining	A01_02	Agriculture, hunting, forestry
Agriculture and Mining	A03	Fishing and aquaculture
Agriculture and Mining	B07_08	Mining and quarrying, non-energy producing products
Agriculture and Mining	B09	Mining support service activities
Fossil fuel energy	B05_06	Mining and quarrying, energy producing products
Non-durable manufacturing	C10T12	Food products, beverages and tobacco
Non-durable manufacturing	C13T15	Textiles, textile products, leather and footwear
Non-durable manufacturing	C16	Wood and products of wood and cork
Non-durable manufacturing	C17_18	Paper products and printing
Non-durable manufacturing	C19	Coke and refined petroleum products
Non-durable manufacturing	C20	Chemical and chemical products
Non-durable manufacturing	C21	Pharmaceuticals, medicinal chemical and botanical products
Non-durable manufacturing	C22	Rubber and plastics products
Non-durable manufacturing	C23	Other non-metallic mineral products
Non-durable manufacturing	C24	Basic metals
Non-durable manufacturing	C25	Fabricated metal products
Durable manufacturing	C26	Computer, electronic and optical equipment
Durable manufacturing	C27	Electrical equipment
Durable manufacturing	C28	Machinery and equipment, nec
Durable manufacturing	C29	Motor vehicles, trailers and semi-trailers
Durable manufacturing	C30	Other transport equipment
Durable manufacturing	C31-C33	Manufacturing nec; repair and installation of machinery and equipment
Service	D -T	Other sectors

B.3 Data for Section 2.1

This appendix documents the data used in Section 2.1.

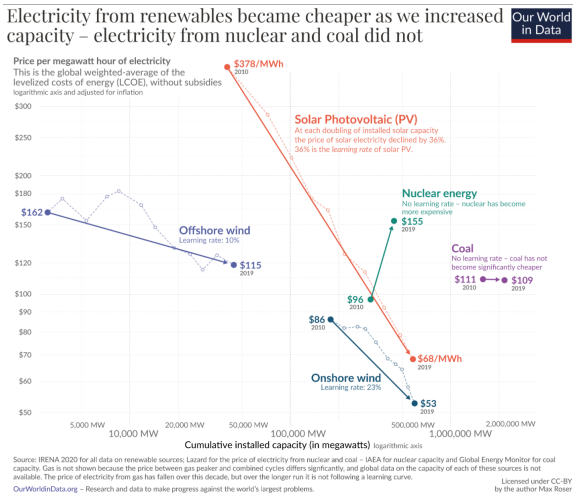
Panel (a) of Figure 1 (U.S. import penetration). For solar, I use the U.S. Energy Information Administration's *Monthly Solar Photovoltaic Module Shipments* to proxy domestic supply and compute import penetration as the share of imports in total U.S. supply.[2] For wind, I use the U.S. Department of Energy's *Land-Based Wind Market Report*, which reports domestic-content shares by major component (nacelle assembly, towers, blades/hubs). I aggregate these component shares using component value-cost weights to obtain a plant-level domestic-content measure and the implied import share.

Panels (b) and (c) of Figure 1 (trade flows and production). Bilateral trade data come from UN Comtrade at the 6-digit HS level. For solar equipment I use HS `854140` (photosensitive semiconductor devices, including PV cells and modules, and LEDs). For wind equipment I use HS `850231` (wind-powered generating sets) and `850300` (parts of electric motors/generators). I also include `841290` (parts of engines and motors) to capture additional wind components.s Solar equipment production comes from the IEA PVPS dataset. For wind production in 2021, I apportion by each country's share of value added in the global wind supply chain using Global Wind Energy Council (2023).

Panel (d) of Figure 1 (equipment price). Solar equipment price time series is taken from the IEA PVPS module price series. For wind equipment, I use IRENA's global onshore wind cost index.

[2] "Import penetration" is measured as the import share in total U.S. supply.

Figure B.1: Price of Electricity by Source



Source: Our World in Data

B.4 Data Construction in LBD Estimation (Section 4.4)

This section details the construction of $c^j_{n,t}$, $\pi^j_{nn,t}$, and $P^j_{n,t}$ used to invert (24). For input costs $c^j_{n,t}$, I use data from the Penn World Table (Version 10.1). I assume that input costs are composed of wages ($w_{n,t}$), manufacturing goods, and services. I calculate $w_{n,t}$ as the ratio of total labor compensation to total employment (using the variable emp in PWT), where labor compensation is the product of labor share (variable $labsh$) and GDP (variable $cgdpo$). I proxy the manufacturing price index using the average of a country's import and export prices (variables pl_m and pl_x, respectively). For the service price index, I use the consumer price index (CPI).

For solar energy equipment, I obtain the output $y^S_{n,t}$ and price data $P^S_{n,t}$ from International Energy Agency Photovoltaic Power Systems Programme (PVPS). PVPS provides historic price and quantity of solar energy equipment in major countries. I construct the domestic expenditure share sequence $\pi^S_{nn,t}$ by combining export data from Comtrade and output and price data from PVPS. That is, I compute total value of production for solar by multiplying output by price from PVPS and then subtract the total value of export from Comtrade.

For wind energy equipment, there is no available time-series data for global production. To recover the annual output, I follow the following steps. First, I use annual wind energy equipment installation data (in GW) and the average installation cost for each country from IRENA, assuming a one-year time lag between the production/trade and installation of renewable energy equipment. Using this installation data and the average installation costs, I compute the annual absorption of wind energy equipment. By combining wind equipment import data from Comtrade with the absorption data, I derive the domestic expenditure share sequence, $\pi^W_{nn,t}$. Lastly, I use wind energy equipment export data from Comtrade, along with the absorption data, to calculate production in each country.

This approach allows me to impute annual wind energy equipment output despite the absence of country-level time-series production data.

B.5 Renewable Potential

B.5.1 Geospatial Data for Renewable Potential

Although renewable energies are often considered 'infinite,' the amount of energy that can be generated in any given location depends on the region's renewable potential. Furthermore, even areas with high potential may not be suitable for installing renewable energy infrastructure. Oakleaf et al. (2019) introduced the Development Potential Index (DPI) at a 1 km resolution, utilizing spatial multi-criteria decision analysis within geographic information systems. They first identified sector-specific land constraints that could restrict development, such as appropriate land cover and slope. Then, they developed spatially explicit criteria—continuously scaled factors that improved the suitability of a region for development. These criteria accounted for both renewable potential and development feasibility, considering factors such as proximity to major roads, railroads, ports, power plants, the electrical grid, and demand centers.

Figure B.2 shows the global distribution of renewable energy potentials, specifically solar and wind, across the entire globe (panel (a) and (b)), using data from the Global Solar and Wind Atlas, as well as across regions that consider the feasibility of development (panel (c) and (d)), based on Oakleaf et al. (2019). In all panels, regions shown in red have higher potential, while regions colored blue have lower potential. There is significant heterogeneity not only between countries but also within each country.

Two patterns emerge: First, within-country heterogeneity in renewable energy potentials increases when development feasibility is factored in, and second, the feasible areas for installing renewable energy equipment are quite limited—especially for wind energy, which has a smaller feasible area compared to solar energy. I incorporate these spatial feasibility and potential measures directly into the model and calibrate the corresponding parameters.

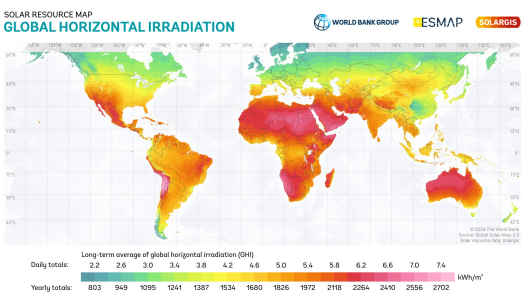
B.5.2 Alternative Method to Calibrate DRS

In this section, I present an alternative way to calibrate diminishing returns in renewable-energy production by combining solar and wind farm location data with time-invariant resource-potential maps. While the resource potential at a given site is fixed, the set of installed solar and wind farms evolves over time. Using each plant's commissioning (start) year and coordinates (longitude and latitude), I compute, for each country and year, the *average* resource potential of the locations actually installed.

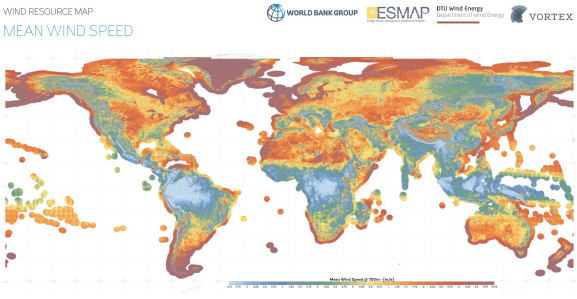
Figure B.4 illustrates how deployment maps to resource quality using two snapshots. Panel (a) shows the locations of solar farms operating in 2011. Panel (b) overlays 2022 solar-farm locations on the global solar-potential map (darker shading indicates lower potential). Using the dataset's annual

Figure B.2: Renewable Potentials

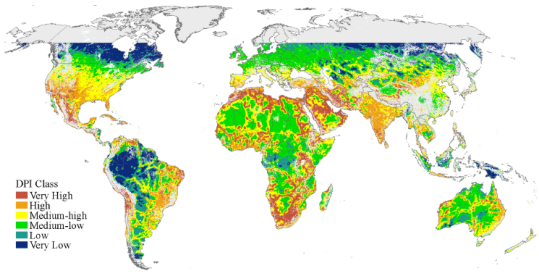
(a) Solar Potential



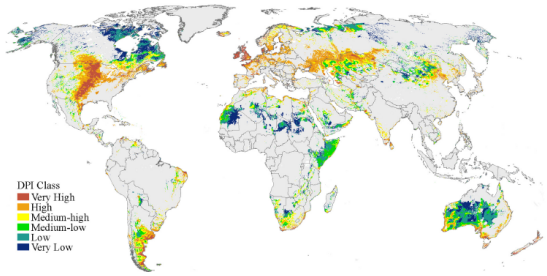
(b) Wind Potential



(c) DPI (Solar)



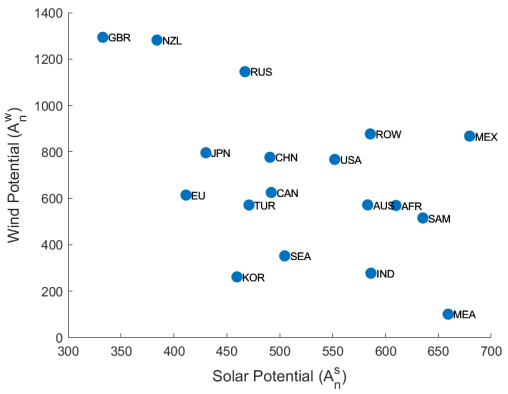
(d) DPI (Wind)



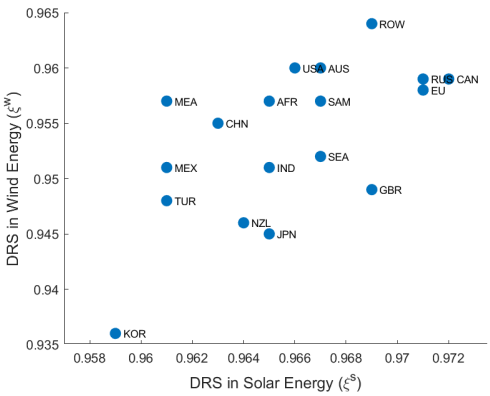
Note: Panel (a) displays solar potential measured by global horizontal irradiation across the world. (b) depicts wind potential measured by mean wind speed at 100m height across the world. Panel (c) and (d) displays the Development Potential Index (DPI) of solar and wind, respectively. Source: Panel (a): Global Solar Atlas, panel (b): Global Wind Atlas, panel (c) and (d): Oakleaf et al. (2019).

Figure B.3: Renewable Potentials and DRS in Renewable Energy Production

(a) Renewable Potentials (A_n^s)



(b) Decreasing Return to Scale (ζ_n^s)

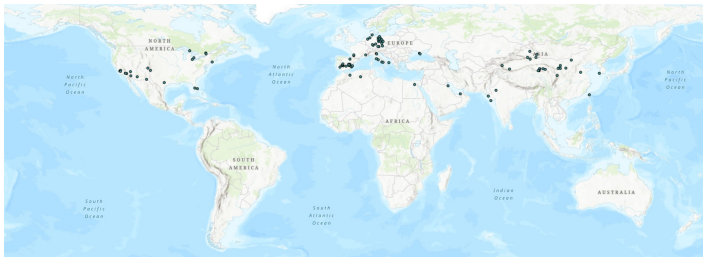


Note: Panel (a) displays country-level solar and wind potentials measured by global horizontal irradiation. Panel (b) depicts the measured decreasing returns to scale parameter in solar and wind energy productions.

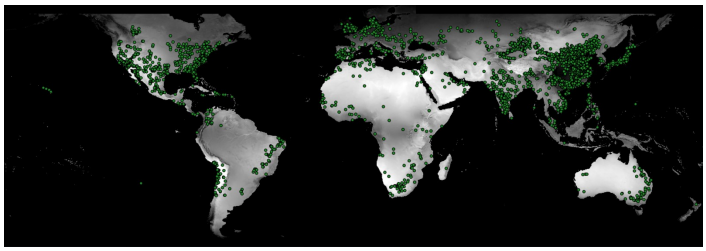
additions, I track how the average resource quality of utilized sites changes over time within each country.

Figure B.4: Combining Renewable Power Farm and Renewable Potential Data

(a) Solar Power Farm Location in 2011



(b) Combining Solar Potential and Solar Power Farm Location in 2022



Panel (a) shows the locations of solar farms operating in 2011. Panel (b) overlays 2022 solar-farm locations on the global solar potential map (darker shading denotes lower potential).

Formally, for each $j \in \Omega_{RE}$, I estimate the relationship between average site potential and cumulative installations by regressing the average potential of installed locations in country n and year t on cumulative installed capacity:

$$\log\left(A^{j}_{n,t}\right) \;=\; \xi^{j,\mathrm{ALT}} \log\left(K^{j}_{n,t}\right) \;+\; \mathrm{FE}^{j}_{n} \;+\; \varepsilon^{j}_{n,t}, \tag{B.1}$$

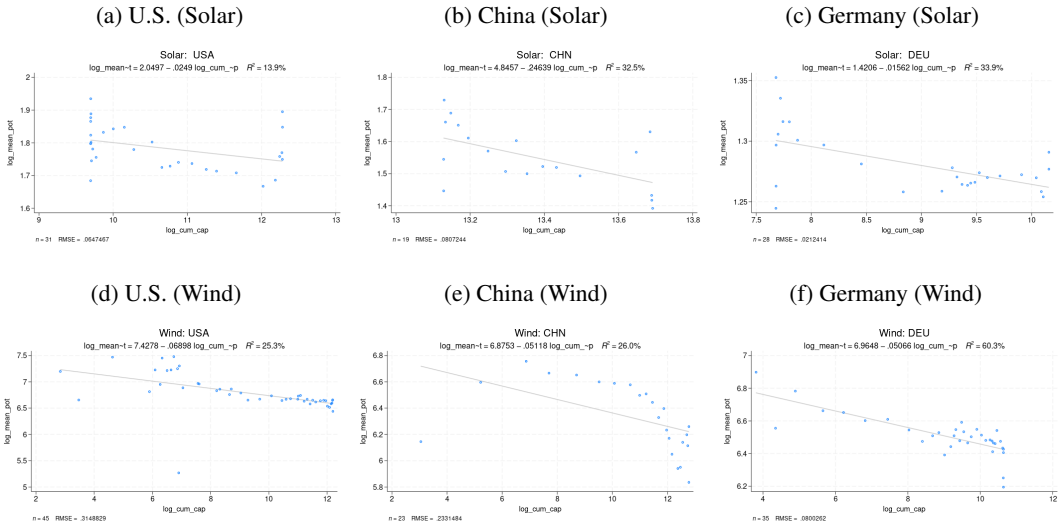
where $A^{j}_{n,t}$ is the (country–year) average resource potential at installed sites, $K^{j}_{n,t}$ is cumulative installations, and FE^{j}_{n} are country fixed effects.[3] A negative $\xi^{j,\mathrm{ALT}}$ indicates that, as cumulative installations rise, developers progressively move to lower-potential sites (diminishing renewable potential).

Table B.2 reports the estimated correlations for major countries after controlling for country fixed effects.[4] Two results emerge. First, average site potential declines with additional installations for both solar and wind. Second, the decline is steeper for wind than for solar, consistent with the main DPI-based specification. In magnitude, the patterns are broadly similar to the DPI measure, with DPI implying a slightly faster diminishing return for solar and a somewhat slower one for wind.

[3] The renewable potential at each grid cell is constant; however, the average potential of installed sites evolves as new sites are added.

[4] Figure B.5 visualizes these relationships country by country for solar and wind.

Figure B.5: Estimating Decreasing Return to Scale in Renewable Energy Production



Note: This figure plots the relationship between the log of annual cumulative renewable energy equipment installation on x-axis and the log of renewable potential in newly installed locations on y axis. Panel (a)-(c) plot the case for solar in the US, China, and Germany, and (d)-(f) plot the case for wind for corresponding countries.

B.6 Measuring Initial Capital Stocks

I measure initial capital stocks for each asset type (fossil fuel, solar, wind, and non-energy) as follows:

1. **Aggregate capital.** I construct each country's total capital stock using the Penn World Table, which reports capital stocks normalized to the U.S. level. I scale each country's value by the U.S. level to obtain absolute amounts.[5]

[5]Capital Stock at Constant National Prices for the United States, retrieved from FRED, Federal Reserve Bank of St. Louis; https://fred.stlouisfed.org/series/RKNANPUSA666NRUG, June 29, 2024.

Table B.2: Additional Evidence of DRS

	$\zeta^{s,ALT}$	$\zeta^{w,ALT}$
$log(K^s_{n,t})$	-0.012**	
	(0.0038)	
$log(K^w_{n,t})$		-0.071***
		(0.0083)
FE	✓	✓
N	949	1163

Standard errors in parentheses

* $p < 0.05$, ** $p < 0.01$, *** $p < 0.001$

2. **Fossil fuel capital.** I take nominal capital by industry from the WIOD Socio-Economic Accounts. For countries not covered by WIOD but included in my analysis, I impute fossil fuel capital using the average ratio of fossil fuel capital to fossil fuel output from the WIOD dataset.
3. **Solar and wind capital.** I convert installed capacity (kW) into dollar values. As of 2021, the global capital value of wind farms (USD 2.22 trillion) is taken from industry estimates.[6] I first recover gross capital stock using a cumulative depreciation rate, and then allocate this capital stock across countries according to each country's share of global wind installations (in kW). Similarly, assuming the same depreciation rate for solar and wind energy equipment, I derive the capital stock for installed solar energy equipment based on the relative global share of installed solar to wind capacity (approximately 1.26:1). Applying the same distribution method, I estimate each country's initial stock of capital for solar energy equipment.
4. **Non-energy capital.** I compute non-energy capital as the residual: aggregate capital minus the sum of fossil fuel, solar, and wind capital.

B.7 Calibrating the Damage Parameter

Following Caliendo et al. (2024), I map the EPA social cost of carbon (SCC) into the model's damage parameter so that, at the baseline allocation, the model-implied *marginal* welfare loss from an extra ton emitted in year t equals the EPA SCC_t (in constant dollars and CO_2e units). Here, the social cost of carbon differs across time. To incorporate that in the calibration, I do the following.

Aggregating multiple gases to a single CO_2-equivalent price. Starting from the EPA (2023)'s annual, per-ton global damage schedules for CO_2, CH_4, and N_2O (2% near-term Ramsey discount rate), I express each gas on a CO_2-equivalent basis using 100-year global warming potentials (GWP_{100}) and then aggregate those. For gas $g \in \{CO_2,\ CH_4,\ N_2O\}$ in year t, let $\text{SC}_g(t)$ denote the social cost per metric ton of that gas and GWP_g (with $\text{GWP}_{CO_2} = 1$). The per-ton CO_2e price for gas g is $\text{SC}_g(t)/\text{GWP}_g$. To obtain a single CO_2e price, I take a weighted average across gases using a fixed emissions mix with weights w_g that sum to one:

$$\text{SC-CO}_2\text{e}(t) \;=\; \sum_{g\in\{CO_2,\ CH_4,\ N_2O\}} w_g \cdot \frac{\text{SC}_g(t)}{\text{GWP}_g}.$$

This yields a single $\$/\text{tCO}_2\text{e}$ for each year from 2020 through 2080 that is consistent with gas-specific damages under the specified mix (researchers should substitute their inventory's gas shares if they differ). For illustration, the social cost of carbon years are $\$175/\text{tCO}_2\text{e}$ in 2021, \$206 in 2030, \$283 in 2050, and \$382 in 2080. After 2080, I assume the social cost of carbon is flat at \$382.

Country-specific Social Cost of Carbon. As a robustness check, I do the same IRA exercise

[6] https://www.chaucergroup.com/news/total-capital-value-of-wind-farms-worldwide-reaches-19tn.

when the damage parameter differs across time and countries, i.e., $SCC_{n,t}$. The results are in Appendix Section C.10. Here I explain how to incorporate country heterogeneity. To keep the EPA's global SC_{GHG} level and time path intact while introducing geographic heterogeneity, I map EPA's per-ton series to countries using country-level social cost of carbon (CSCC) from Ricke et al. (2018).[7] One caveat of this dataset is that the CSCC is strongly correlated with population in each country. To resolve this, for each country c, I compute the per-capita CSCC as $\text{pcCSCC}_c \equiv \text{CSCC}_c / \text{Pop}_c$ from the database. The country multiplier is then

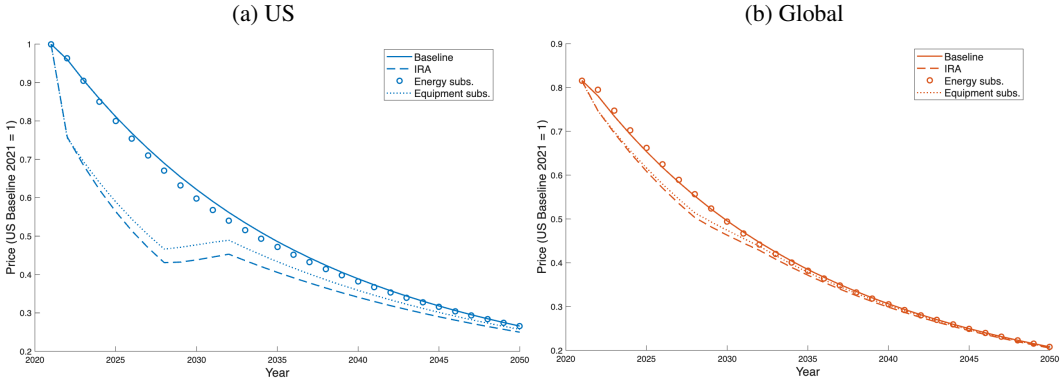
$$m_i \equiv \frac{\text{pcCSCC}_i}{\sum_j \text{pcCSCC}_j}, \quad \text{SCC}_i = m_i \times \text{SCC}^{EPAGlobal}$$

so the population-weighted average of $\{m_c\}$ equals 1 by construction. Then I distribute EPA's aforementioned annual social cost of carbon to each country using the country multiplier. By doing so, I match the aggregate social cost of carbon to EPA and obtain heterogeneity across countries.

Appendix C Additional Results

C.1 Impact of Subsidies on Wind Equipment Price

Figure C.1: Wind Equipment Price



Note: Each panel plots the effect of subsidies on wind equipment price, in the U.S. (panel (a)) and the aggregated global (panel (b)). Baseline price is plotted by blue solid line, price under IRA is plotted by red dashed line, energy subsidy by yellow circles, and equipment subsidy by purple dotted line.

Figure C.1 shows how the energy, equipment, and combined IRA subsidies affect wind-equipment prices in the U.S. (panel (a)) and globally (panel (b)). Relative to the solar-equipment results (Figure 4), the wind-equipment price shows two key differences. First, in the U.S. (Panel (a)), the energy sub-

[7] To align with EPA's 2% near-term Ramsey discount rate, I use the closest Ricke et al. (2018) specification: growth-adjusted discounting with pure rate of time preference $\rho = 2\%$ and elasticity $\eta = 1.5$, the BHM short-run (pooled) damage function, scenario SSP2/RCP6.0, and the median (50th percentile) statistic.

sidy reduces wind-equipment prices more than it does for solar because a larger share of U.S. wind demand is served by domestic producers; the induced demand is internalized, scales up production, and strengthens learning, pushing unit costs down. Second, globally (Panel (b)), all subsidies yield smaller price declines for wind than for solar, consistent with a lower trade elasticity in wind equipment: supply expansions transmit less across borders, so the equipment subsidy and the IRA have more muted global price effects.

C.2 Estimated Fiscal Cost and Instrument Complementarities

A key result is that the *combined* IRA outlay exceeds the sum of the energy-only and equipment-only outlays because the two instruments are complementary. With the equipment subsidy in place, the energy subsidy's demand surge is met largely by domestic supply, expanding eligible output; conversely, the equipment subsidy lowers unit costs and scales domestic manufacturing, which in turn supports more renewable deployment. These interactions raise total spending relative to running either instrument in isolation.

Quantitatively, the model implies a fiscal cost of $243 billion for the IRA's renewable-energy provisions—above the Congressional Budget Office estimate of $96 billion Congressional Budget Office (2024), and closer to Arkolakis and Walsh (2023) ($160 billion) and the Wharton Budget Model ($263 billion; Penn Wharton Budget Model (2023)). A secondary contributor to higher spending in my framework is that the U.S. can become a net exporter of renewable-energy equipment, which makes some outlays apply to export volumes.

C.3 Who Reduces Carbon Emissions?

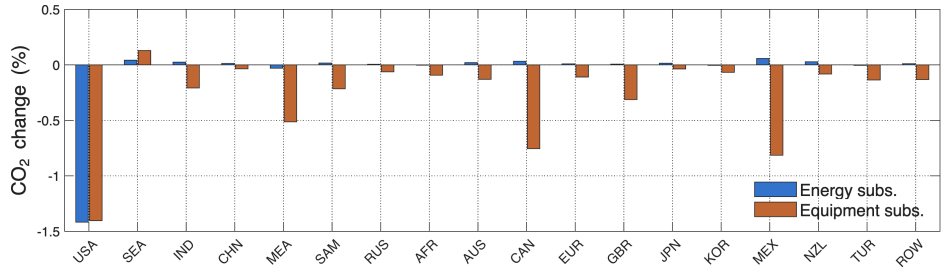
The subsidies' distinct mechanisms generate fundamentally different spillovers for global carbon emissions, summarized in panel (a) in Figure C.2. The energy subsidy concentrates abatement in the U.S. with some carbon leakage to other countries (blue bars); the equipment subsidy (red bars) spreads abatement more broadly by lowering world equipment prices. Blue bars in Panel (b) plots the outcome under combined IRA; the IRA combines these channels to diffuse decarbonization across countries (also see Table C.1). Quantitatively, as summarized in table 6, the energy subsidy lowers global CO_2 by 0.16%, the equipment subsidy by 0.27%. Given that the two instruments use nearly the same budget ($117 and $125 billion, respectively), the equipment subsidy is more efficient in marginal terms. The combined IRA delivers the largest cut at 0.63%, with roughly a quarter of this reduction occurring outside the U.S.

C.4 Welfare Decomposition

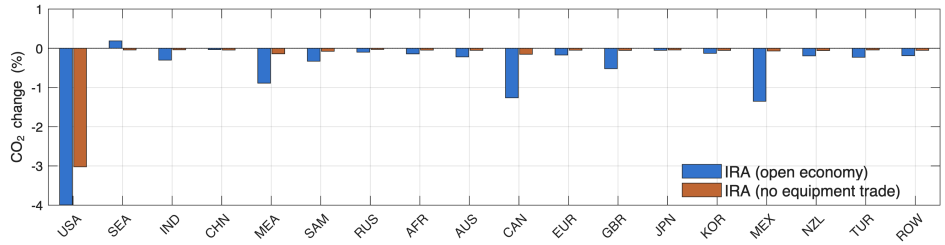
Tables C.1 and C.2 report the welfare decomposition—real income (non-carbon), carbon benefit, and their sum—by group and by country, respectively, with all changes cumulated through 2100. Two

Figure C.2: Geographic Incidence of CO_2 Reductions (Who Abates)

(a) Under Energy / Equipment Subsidies



(b) Under IRA with and without Equipment Trade



Notes: Each panel reports the percent change relative to the baseline in cumulative CO_2 emissions through 2100, by country. Panel (a) shows the individual instruments—energy subsidy (blue bars) and equipment subsidy (red bars); Panel (b) shows the combined IRA under the baseline model (blue bars) and under an alternative model without equipment trade (red bars). Negative values indicate emission reductions; positive values indicate emission increases (carbon leakage).

messages emerge. First, tilting the policy mix toward equipment support raises U.S. real income up to a point, but the global real-income effect is negative as learning and market share shift away from incumbents, where the inefficiency arises—an incidence pattern discussed in the main text.[8] Second, adding the carbon component raises total welfare; in the aggregate, discounted carbon gains are large enough to offset negative real-income effects for the full IRA. These patterns are visible in the group aggregates of Table C.1 and echoed at the country level in Table C.2.

For the U.S., the energy subsidy lowers real income by -0.06% while delivering a small carbon benefit of 0.03%, yielding total welfare of -0.04%; the equipment subsidy flips the sign on real income (0.06%) and, with a similar carbon benefit (0.03%), produces total welfare of 0.08%. Under the full IRA, U.S. real income is slightly negative (-0.01%) but the carbon component is large (0.07%), so total welfare is 0.05%. For equipment exporters (CHN, IND, SEA), energy subsidies raise real income on average (0.01%) while equipment subsidies reduce it (-0.05%), with corresponding total welfare of 0.04% (energy) and -0.02% (equipment); the IRA combines a negative real-income component (-0.06%) with a sizable carbon benefit (0.07%) to yield a near-zero total (0.01%). Fossil-fuel exporters (MEA, SAM, RUS) lose real income under both instruments (energy

[8] Appendix Figure C.2 shows an inverted-U for U.S. real income in the equipment share and a monotonically negative global real-income schedule; higher energy subsidy lines sit lower for the U.S., consistent with demand-side support leaking to foreign producers.

Table C.1: Real Income, Carbon Benefit, and Total Welfare by Group (to 2100, %)

Country Group	Policy	Real Income (%)	Carbon Benefit (%)	Welfare (%)
United States (USA)	Energy subs.	-0.06	0.03	-0.04
	Equip. subs.	0.06	0.03	0.08
	IRA	-0.01	0.07	0.05
Equip. Exporters (CHN, IND, SEA)	Energy subs.	0.01	0.03	0.04
	Equip. subs.	-0.05	0.03	-0.02
	IRA	-0.06	0.07	0.01
Fossil Fuel Exporters (MEA, SAM, RUS)	Energy subs.	-0.02	0.03	0.01
	Equip. subs.	-0.04	0.03	-0.01
	IRA	-0.08	0.07	-0.00
Global Aggregate	Energy subs.	0.00	0.03	0.03
	Equip. subs.	-0.03	0.03	-0.00
	IRA	-0.04	0.07	0.03

Notes: Values are percentage changes (e.g., 0.081 means 0.081%). Group entries are simple (unweighted) means across members of the 18-country set: AFR, AUS, CAN, CHN, EUR, GBR, IND, JPN, KOR, MEA, MEX, NZL, RUS, SAM, SEA, TUR, USA, ROW. "Carbon Benefit" is the welfare contribution from reduced emissions; "Real Income" is the non-carbon component; "Total Welfare" is their sum.

-0.02%, equipment -0.04%) but carbon gains partly offset these, leaving welfare near zero for energy (0.01%) and slightly negative for equipment (-0.01%); the IRA again shows a large carbon benefit (0.07%) against a real-income loss (-0.08%), netting to roughly 0.00%. At the global aggregate, energy's real income is 0.00% and welfare 0.03%, whereas equipment's real income is -0.03% and welfare $\approx$ 0.00%; the IRA shows a global real-income loss of -0.04% more than offset by a 0.07% carbon benefit, yielding global welfare gain of 0.03%. Country-level entries are in Table C.2.

C.5 Optimal Subsidy

In this section, I examine how reallocating a fixed IRA budget between energy and equipment subsidies alters U.S. and global welfare—decomposed into real-income and carbon components—with Figure C.3 Panel (a) reporting real-income effects and Panel (b) adding the carbon benefit.

Mix of instruments: real-income effects. Panel (a) in Figure C.3 traces real-income responses as the subsidy mix tilts from energy toward equipment, holding the total fiscal outlay fixed. The U.S. real-income effect under equipment subsidy is inverted-U shaped: modest equipment shares reduce domestic unit costs and scale up learning-by-doing, raising U.S. real income, but the gains taper at higher shares and eventually bend down as diminishing returns and fiscal incidence mount. By contrast, the global real-income effect is monotonically negative in the equipment share—a stark *beggar-thy-neighbor* pattern driven by displaced incumbent exporters and redirected learning abroad.

Table C.2: Welfare Decomposition by Country: Energy, Equipment, and IRA (to 2100)

	IRA			Energy subsidy only			Equipment subsidy only		
Country	Welfare (%)	Real Inc. (%)	Carbon (%)	Welfare (%)	Real Inc. (%)	Carbon (%)	Welfare (%)	Real Inc. (%)	Carbon (%)
AFR	0.03	-0.04	0.07	0.03	0.01	0.03	0.00	-0.03	0.03
AUS	0.11	0.04	0.07	0.03	0.00	0.03	0.05	0.03	0.03
CAN	0.10	0.03	0.07	-0.01	-0.04	0.03	0.08	0.05	0.03
CHN	0.05	-0.02	0.07	0.04	0.01	0.03	0.01	-0.02	0.03
EUR	0.08	0.01	0.07	0.03	0.00	0.03	0.03	0.00	0.03
GBR	0.11	0.04	0.07	0.03	0.00	0.03	0.05	0.02	0.03
IND	0.00	-0.07	0.07	0.03	0.01	0.03	-0.02	-0.05	0.03
JPN	0.09	0.01	0.07	0.03	0.00	0.03	0.04	0.01	0.03
KOR	0.09	0.02	0.07	0.04	0.01	0.03	0.03	0.00	0.03
MEA	-0.10	-0.18	0.07	-0.02	-0.05	0.03	-0.06	-0.09	0.03
MEX	0.20	0.13	0.07	0.08	0.05	0.03	0.07	0.04	0.03
NZL	0.12	0.04	0.07	0.03	0.01	0.03	0.05	0.03	0.03
RUS	0.03	-0.05	0.07	0.01	-0.01	0.03	0.01	-0.02	0.03
SAM	-0.14	-0.21	0.07	0.00	-0.03	0.03	-0.09	-0.12	0.03
SEA	-0.06	-0.13	0.07	0.04	0.01	0.03	-0.07	-0.10	0.03
TUR	0.08	0.01	0.07	0.03	0.00	0.03	0.03	0.00	0.03
USA	0.05	-0.01	0.07	-0.04	-0.06	0.03	0.08	0.06	0.03
ROW	0.06	-0.01	0.07	0.03	0.01	0.03	0.02	-0.01	0.03

Consistent with the U.S. being a net equipment importer, higher energy subsidies—compare the red solid, dotted, and dashed lines—lower U.S. real income: demand-side support leaks to foreign producers via import pass-through, so the U.S. bears fiscal costs while real-income gains accrue overseas.

Adding carbon benefits. Panel (b) incorporates the carbon component and shows how the welfare ranking shifts as equipment support rises. Because a more equipment-tilted mix compresses global equipment prices and accelerates deployment, the resulting global CO_2 reduction grows with the equipment share and progressively offsets the negative global real-income effect. Quantitatively, global welfare begins to rise once the equipment subsidy exceeds about 40%, as the carbon benefit dominates the real-income losses beyond that threshold. For the U.S., however, U.S. welfare is hump-shaped and peaks at an equipment share of 40%: beyond this point, the marginal real-income cost of pushing additional equipment support (after accounting for fiscal incidence) outweighs the incremental gain, making mixes above 40% too costly for the U.S. in welfare terms.

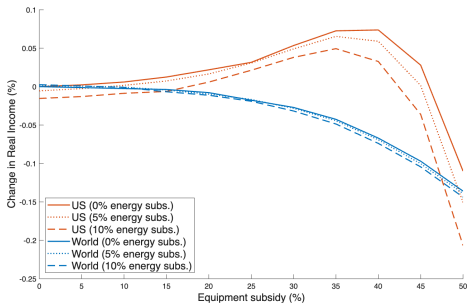
C.6 The Role of Equipment Trade for Individual Subsidies

While the main text focuses on the full IRA, this section details how the absence of equipment trade alters the effects of the energy and equipment subsidies individually. The results, summarized in Table C.3, are starkly different from the baseline model with trade.

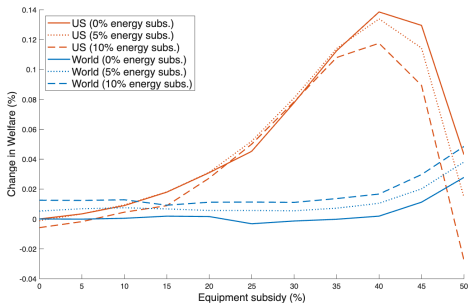
Three patterns are noteworthy. First, without equipment trade the *energy subsidy* becomes more

Figure C.3: Welfare by Subsidy Ratio

(a) Real Income Effect



(b) Total Welfare



Note: This figure plots the relative change in welfare under different subsidy ratios. U.S. welfare is plotted with solid line and global welfare is plotted with dotted line in each panel. This figure plots the percent change in welfare under different combinations of energy and equipment subsidies, holding the policy duration to 10 years. The horizontal axis varies the *ad valorem* equipment subsidy rate, while different lines correspond to varying energy subsidy rates (0%, 5%, and 10%). Panel (a) plots real income component of U.S. welfare (red lines) and aggregate global welfare (blue lines). All changes are cumulative through 2100 relative to the no-policy baseline.

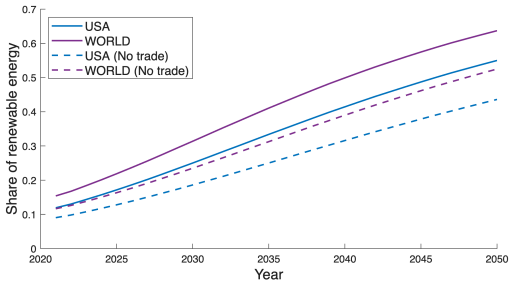
effective at reducing global CO_2 than the equipment subsidy (-0.15% vs. -0.13%). Second, while global welfare under the energy subsidy changes little, global welfare under the *equipment subsidy* turns positive (0.02% vs. -0.00% with trade). The reason is that the beggar-thy-neighbor channel of the equipment subsidy disappears: foreign producers are no longer displaced from equipment markets, so productivity gains abroad are not suppressed. Third, for U.S. welfare, the energy subsidy's negative effect largely vanishes in the no-trade case (-0.00% vs. -0.04% with trade) because additional domestic demand is now met by U.S. equipment producers, which fosters learning-by-doing at home rather than abroad.

Table C.3: Welfare Comparison for Individual Subsidies

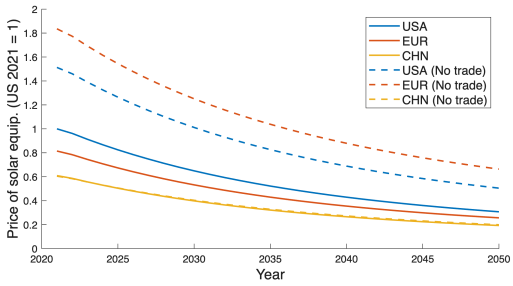
Scenario	Subsidy Type	Global CO_2 (%)	Global Welfare (%)	U.S. Welfare (%)
Baseline (with trade)				
	Energy Subs.	-0.16	0.03	-0.04
	Equipment Subs.	-0.27	-0.00	0.08
No equipment trade				
	Energy Subs.	-0.15	0.03	-0.00
	Equipment Subs.	-0.13	0.02	0.08

Figure C.4: Role of Renewable Energy Equipment Trade

(a) Share of Renewable Energy



(b) Price of solar equipment



Note: Panel (a) shows the share of renewable energy in total primary energy use from 2021 to 2050 in the U.S. (blue) and globally (purple). Panel (b) shows the solar-equipment price index over the same period in the U.S. (blue), the EU (red), and China (yellow). Solid lines denote the baseline with calibrated trade costs; dashed lines denote the no-trade counterfactual for renewable-energy equipment.

C.7 Comparative Statics

C.7.1 Role of renewable energy equipment trade

To assess the role of renewable energy equipment trade in the transition, I compare the baseline scenario with calibrated trade costs to a scenario with no trade. In the no trade scenario, I eliminate trade in renewable energy equipment by setting the trade cost to infinity, i.e., $d^j_{in,t} = \infty$ for $j \in S, W$ and $i \neq n$.

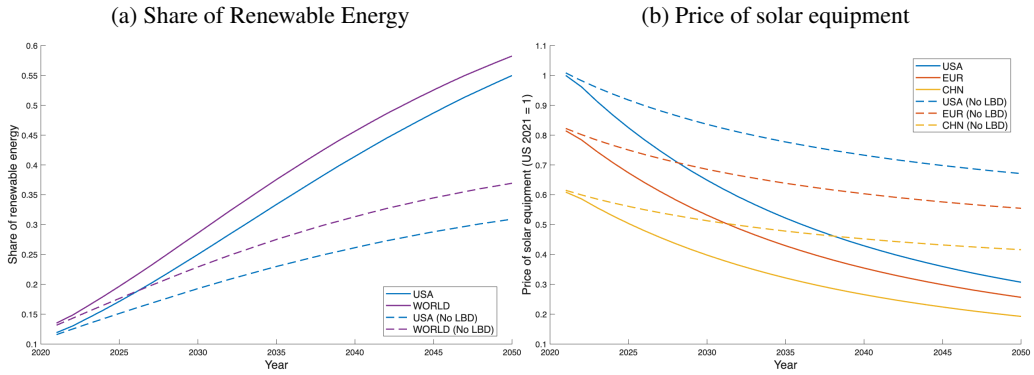
Panel (a) of figure C.4 compares the share of renewable energy in the U.S. and globally under the current calibration and under no trade scenario. In the baseline scenario, represented by the solid line, the share of renewable energy in primary energy use reaches 49% in the U.S. and 53% globally. In contrast, Without trade, the share of renewable energy in primary energy use only reaches 38% in the U.S. and 40% globally (dashed lines). These outcomes are driven by the equipment price trends shown in Panel (b).

Panel (b) shows the evolution of the price index for solar energy equipment from 2021 to 2050 in the US, EU, and China under each scenario. In the no trade scenario, the price spikes in the U.S. and EU, while the increase in China is relatively small, as China has been the main exporter under the baseline. Overall, higher equipment prices in the no equipment trade scenario discourages investment in renewable energy in each country, slowing the energy transition.

C.7.2 Role of learning-by-doing in the transition

A key component of the model is learning-by-doing in renewable-equipment production. To assess its impact, I shut down learning-by-doing by setting $\nu^S_D = \nu^W_D = 0$ and re-simulate the transition path. Panel (a) of Figure C.5 compares the renewable-energy share in the U.S. and global from 2021 to 2050 with and without learning-by-doing. With learning-by-doing enabled, the renewable share

Figure C.5: Role of Learning-by-doing



Note: Panel (a) plots the share of renewable energy in total primary energy use from 2021–2050 for the U.S. (blue) and the world (purple). Panel (b) shows the price index for solar equipment over the same period in the U.S. (blue), the European Union (red), and China (yellow). Solid lines denote the baseline with learning-by-doing; dashed lines shut down learning-by-doing.

in primary energy reaches about 50% in the U.S. (and 55% globally) by 2050; without learning-by-doing, it reaches only about 26% in the U.S. (and 33% globally).

Panel (b) displays the evolution of solar equipment prices in the U.S., the European Union, and China. In the absence of learning-by-doing, equipment-price indexes fall much more slowly because there is no endogenous productivity growth. The muted cost declines depress investment relative to the baseline, producing a markedly slower transition in each country.

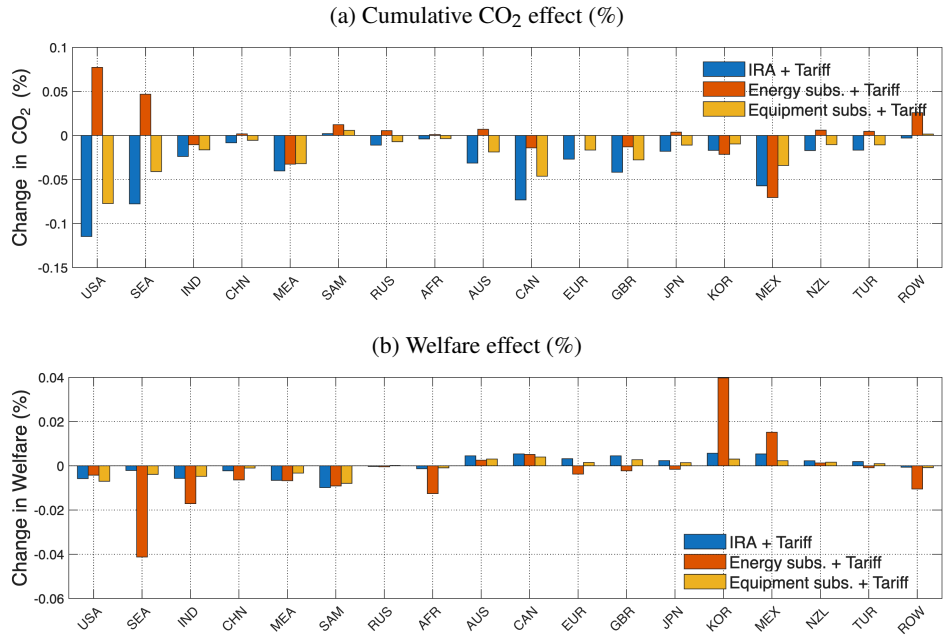
C.8 Additional Results on IRA under Trade Policy

Figure C.6 compares cumulative CO_2 reduction (panel a) and welfare change (panel b) across countries when a U.S. solar-equipment tariff is layered on top of each subsidy scenario, relative to the no-tariff counterpart.

Energy subsidy + tariff. Adding the tariff *weakens* the carbon benefit of an energy-only subsidy by raising delivered equipment prices in the U.S., which slows installations. Consistent with Table 8, this results in a smller global CO_2 reduction (about -0.15% with the tariff vs. -0.16% without), lower global welfare (roughly 0.02% vs. 0.03%) and U.S. welfare (about -0.04%). The mechanism is twofold: higher U.S. prices blunt the domestic transition, and reduced exports from major producers (e.g., Southeast Asia, China) dilute learning-by-doing abroad.

Equipment subsidy + tariff. Pairing the tariff with an equipment subsidy raises U.S. equipment prices in the short run, which can temporarily lift U.S. emissions, but it slightly *strengthens* the long-run global CO_2 reduction (about -0.28% vs. -0.27% without the tariff) and leaves global welfare essentially unchanged (about 0.00% in both cases). The tariff shifts market share toward U.S. producers, reinforcing domestic learning-by-doing and supporting exports; this channel helps offset the tariff's static distortion.

Figure C.6: Welfare and Carbon Effects of IRA with a Solar Tariff Across Countries



Notes: Panel (a) plots the effect of adding a U.S. solar-equipment tariff to each subsidy scenario on cumulative CO_2 emissions by 2100, *relative to the same scenario without the tariff.* Panel (b) plots the corresponding welfare effects for residents in each country.

IRA + tariff. When the tariff is layered onto the full IRA mix, aggregate impacts are very close to IRA alone: global CO_2 falls by about -0.66% vs. -0.63% under IRA, and global and U.S. welfare are practically unchanged (both $\approx 0.03\%$ and 0.05%, respectively). In net, the tariff's price distortion is largely offset by IRA subsidies, while a modest reallocation toward U.S. production nudges market share up.

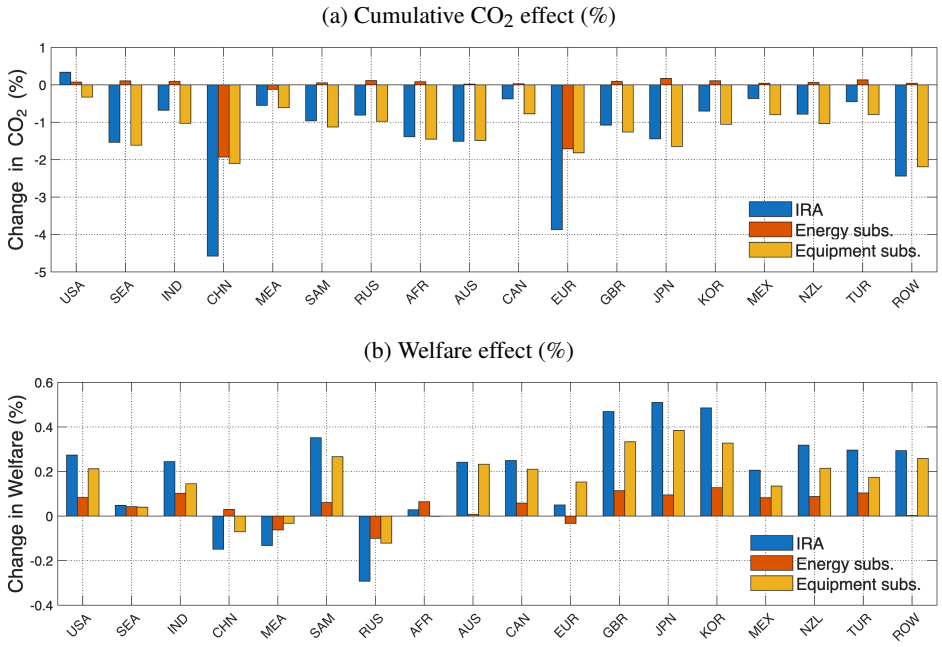
Non-U.S. impacts and third-country effects. Countries directly targeted by the tariff (e.g., China, Southeast Asia) experience the largest welfare losses due to reduced exports and slower learning. Some third countries (e.g., Korea, Mexico) can gain modestly by diverting exports toward the U.S. market. These patterns line up with the small but systematic differences reported in Table 8.

C.9 Additional Results on U.S.-China-EU Policy Competition

The welfare and carbon implications of a joint U.S.–China–EU IRA are heterogeneous across countries. Figure C.7 reports country-by-country changes in cumulative CO_2 and welfare, *each measured relative to its U.S.-only mirror policy* (e.g., the U.S.–China–EU IRA is benchmarked against the U.S.-only IRA, and likewise for energy-only and equipment-only cases).

When China and the EU adopt the same policy as the U.S., U.S. CO_2 emissions decline *less* than under the U.S.-only case because multilateral subsidies depress global fossil-fuel prices, inducing leakage back toward fossil use in the U.S. Nevertheless, the overall effect is strongly favorable for

Figure C.7: Welfare and Carbon Effects of U.S.–China–EU Policies Across Countries



Notes: Panels plot the change in cumulative CO_2 by 2100 (panel (a)) and welfare (panel (b)) across countries when the U.S., China, and the EU implement IRA-like policies. Each bar is measured *relative to the corresponding U.S.-only (mirror) policy:* U.S.–China–EU IRA vs. U.S.-only IRA; U.S.–China–EU energy subsidy vs. U.S.-only energy subsidy; U.S.–China–EU equipment subsidy vs. U.S.-only equipment subsidy.

the climate: the induced cost declines and adoption outside the U.S. spread emissions reductions globally and more than offset the domestic leakage.

Under the joint IRA, the aggregate CO_2 reduction is much larger than in the U.S.-only case (about -2.97% vs. -0.63%), with most direct cuts in the three implementing blocs and additional spillovers via cheaper traded equipment. On welfare, the joint policy raises global welfare (about 0.14%) and U.S. welfare (about 0.33%) on net, though distributional effects vary: fossil fuel exporters tend to lose as global demand falls, while net importers (e.g., Japan, Korea) gain from improved terms of trade and faster adoption. In particular, China and Europe experience significant welfare losses, primarily due to the scale of equipment subsidies. These welfare losses stem from the fact that China already holds 82% of the global solar equipment market share, leaving little room for additional gains through further subsidization. Although the equipment subsidy accelerates the global energy transition by reducing fossil fuel demand, this leads to welfare losses for fossil fuel-exporting countries, such as the Middle East, Russia, and South America. On the other hand, net fossil fuel importers, like Japan and Korea, benefit from the reduced demand for fossil fuels.

C.10 Robustness Check

The impact of the IRA primarily depends on five key sets of parameters: (i) the elasticity of substitution between renewable energy and fossil fuels, η_e, (ii) the (local and global) rates of learning-by-doing in equipment production, ν_D^S and ν_D^W, (iii) the trade elasticities of equipment (θ^S and θ^W), (iv) damage parameter (SCC_t). In this section, I analyze how variations in these parameters influence the outcomes of the IRA.

Higher Elasticity of Substitution Between Renewables and Fossil Fuels. In this scenario, I simulate the IRA with a higher elasticity of substitution between renewables and fossil fuels, setting ψ to 5, compared to the baseline value of $\psi = 3.08$.

Panel (b) in Table C.4 summarizes the results for $\psi = 5$. I find the baseline qualitative patterns persist: the IRA leads to global welfare losses, and the equipment subsidy reduces global carbon emissions more effectively than the energy subsidy. Additionally, the equipment subsidy decreases other countries' welfare while boosting U.S. welfare.

With a higher elasticity of substitution, subsidies become more effective in replacing fossil fuels with renewable energy, thus magnifying the impact of subsidies on reducing global carbon emissions. This results in greater welfare gains from the energy subsidy, both for the U.S. and globally. However, the increased elasticity of substitution raises equipment demand, causing the equipment subsidy to generate higher welfare gains for the U.S. while imposing welfare losses on other countries due to the terms-of-trade effect.

Higher Learning-by-Doing. In this scenario, I simulate the IRA with higher learning-by-doing parameters, $\nu_D^S = 1.89$ for solar and $\nu_D^W = 1.25$ for wind equipment, reflecting the higher range of learning rates found in the literature (Bolinger et al., 2022; Covert and Sweeney, 2024).

Panel (c) in Table C.4 summarizes the results under higher learning-by-doing rates. Overall, the IRA improves U.S. welfare by 1.96%, primarily due to gains from equipment subsidies. Notably, the impact of the subsidies is no longer purely transitory. In the steady state, the U.S. continues to dominate the solar equipment market, which has a long-term positive effect on U.S. welfare and a negative effect on global welfare.

Higher learning-by-doing accelerates the energy transition but also leads to higher carbon emissions, driven by the income effect combined with the low elasticity of substitution between renewables and fossil fuels. While the faster transition to renewable energy reduces energy prices and increases overall economic production, this leads to higher emissions, resulting in a backfire effect on global welfare.

Frictionless spillovers of learning-by-doing. Panel (d) in Table C.4 examines the case where learning-by-doing exhibits a frictionless spillover effect across countries, following Arkolakis and Walsh (2023). To model this, I modify the learning-by-doing process in Equation (19) as follows:

$$A^k_{n,t} = \nu^k_n \Big(\sum_n^N \sum_{i=1}^{t-1} (\mu)^i y^k_{n,t-i} \Big)^{\nu^k_G}, \text{ for } k \in \Omega_{REE}.$$

This specification indicates that an increase in *global* equipment output enhances each country's productivity in equipment production. I calibrate the global learning-by-doing elasticity to align with the elasticity values used in Arkolakis and Walsh (2023), which are 35% for solar equipment and 20% for wind equipment ($\nu^S_G = 1.67$ and $\nu^W_G = 0.52$).

Under frictionless global learning-by-doing, learning-driven productivity gains diffuse internationally. Consequently, the IRA delivers modest global gains and a small U.S. loss: global welfare rises by 0.03%, U.S. welfare falls by -0.10%, and global CO_2 declines by 0.27%. With an energy-only subsidy, global welfare increases by 0.04%. This pattern is consistent with Arkolakis and Walsh (2023): when learning spills over globally, pricing the energy margin yields broad welfare gains. However, it differs from their intuition in the sense U.S. welfare is slightly decreasing (-0.01%), without durable rents from learning-by-doing. On the other hand, an equipment-only subsidy leaves global welfare roughly unchanged ($\approx 0.00\%$) and produces a U.S. loss (-0.04%); because learning rents are fully shared across countries, the policy effectively subsidizes foreign productivity and fails to secure a persistent U.S. market-share advantage.

Low equipment trade elasticities. Setting $\theta^S = \theta^W = 2$ (in line with Boehm et al. (2023)) shifts the rankings toward the carbon channel and strengthens the role of energy subsidy.[9] Energy subsidy delivers a larger CO_2 decline (-0.80%) and raises both global and U.S. welfare (about $+0.09\%$ each). Equipment subsidy still reduces CO_2 (-0.62%) but leaves U.S. welfare essentially unchanged ($\approx 0.00\%$) and global welfare slightly negative (-0.01%), consistent with muted international pass-through and limited displacement of incumbents. The IRA blends these forces: CO_2 falls by -1.51%, global welfare rises more than U.S. welfare (0.07% and 0.04%, respectively). Intuitively, lower cross-origin substitutability dampens world price declines and market-share reallocation, weakening the industrial (terms-of-trade/learning) channel while leaving the green (carbon) channel relatively stronger.

Extending Policy Periods. In the baseline IRA scenario, the policy is not strong enough to generate a lasting increase in the U.S. equipment-market share. A natural adjustment is to extend the policy duration. I extend the subsidy window from 10 years (2022–2031) to 20 years (2022–2041) and compare equilibrium outcomes in Panel (f). The longer horizon magnifies CO_2 reductions, raises global welfare, and increases the U.S. share of the global equipment market, but it does not change the qualitative ranking of instruments. However, the IRA now reduces U.S. welfare, primarily because the additional fiscal cost from extending the subsidy period outweighs the incremental gains. Despite

[9] I re-estimate κ^j_{ni} and ν^j_D to re-match baseline bilateral equipment trade shares and cost trajectories, since $\{\kappa^j_{ni}), \nu^j_D\}$ are identified in the gravity–LBD system given θ^j.

larger short-run effects, the impacts remain transitory: once the subsidies expire, the U.S. equipment-market share returns to its initial level.

Heterogeneous Damage Function. Allowing country-specific damages (Panel (g)) leaves the aggregates close to the baseline: global welfare ticks up 0.05 percentage points (from 0.03% to 0.08%), while U.S. welfare is slightly smaller ($\approx$ 0.03%). The distribution shifts, however: countries with higher marginal climate damages—notably India and China—gain more from the carbon-benefit component relative to the homogeneous-damage case, even as global aggregates move little.

Table C.4: Robustness Check

	Global CO_2 (%)	Global Welfare (%)	U.S. Welfare (%)
(a) Baseline Specification			
IRA	-0.63	0.03	0.05
Energy Subs.	-0.16	0.03	-0.04
Equipment Subs.	-0.27	0.00	0.08
(b) Elasticity of Substitution (ψ = 5)			
IRA	-3.17	0.06	0.73
Energy Subs.	-0.97	0.08	0.10
Equipment Subs.	-1.27	-0.03	0.41
(c) Higher Learning Rate ($\nu_D^S = 1.89$, $\nu_D^W = 1.25$)			
IRA	1.71	-0.86	2.43
Energy Subs.	-0.27	-0.01	0.03
Equipment Subs.	3.36	-0.98	1.91
(d) Frictionless Learning-by-doing ($\nu_G^S = 1.67$, $\nu_G^W = 0.52$)			
IRA	-0.27	0.03	-0.10
Energy Subs.	-0.17	0.04	-0.01
Equipment Subs.	-0.08	0.00	-0.04
(e) Equipment Trade Elasticity ($\theta^S = 2$, $\theta^W = 2$)			
IRA	-1.51	0.07	0.04
Energy Subs.	-0.80	0.09	0.09
Equipment Subs.	-0.62	-0.01	0.00
(f) Extending Policy Periods (2022-2041)			
IRA	-2.22	0.12	-0.12
Energy Subs.	-0.55	0.07	-0.13
Equipment Subs.	-1.15	0.04	0.16
(g) Country-level Social Cost of Carbon ($SCC_{n,t}$; Ricke et al. (2018))			
IRA	-0.63	0.08	0.03
Energy Subs.	-0.16	0.05	-0.05
Equipment Subs.	-0.27	0.01	0.08

Appendix D Algorithm

This section describes the algorithm used to solve the model.

To compute the transition path and steady state, I set T sufficiently large to ensure convergence to the steady state. In practice, $T = 200$ suffices.

1. Use the calibrated parameter values $A^j_{n,t}$, σ^j_n, α, $d^j_{in,t}$, $\tau^j_{in,t}$, μ^j_n, $\gamma^j_{n,t}$, $\gamma^{L,j}_{n,t}$, $\gamma^{M,j'j}_{n,t}$, $\gamma^{j',j}_{n,t}$, η^j $\quad \forall\, j,n,t$.[10]
2. Make an initial guess for the investment-rate sequence $\{\varphi^k_{n,t}\}_{n=1,\dots,N;\, t=1,\dots,T}$ for each capital good $k \in \Omega_K$, based on the current stock:

$$I^k_{n,t} \;=\; \varphi^k_{n,t} K^k_{n,t}. \tag{D.1}$$

3. Solve the static problem at each t using the algorithm in Alvarez and Lucas (2007).
   (a) Start in period $t = 1$ with capital endowments (and their allocation) $\mathbf{k}^k_1 \equiv (k^k_{11}, k^k_{21}, \dots, k^k_{N1})$ for all $k \in \Omega_K$.
   (b) Guess factor and energy prices: $\mathbf{w}_1 \equiv (w_{11}, w_{21}, \dots, w_{N1})$, $\quad \mathbf{r}^k_1 \equiv (r^k_{11}, r^k_{21}, \dots, r^k_{N1})$ $\forall k \in \Omega_K$, $\quad \mathbf{P}^j_1 \equiv (P^j_{11}, P^j_{21}, \dots, P^j_{N1})$ $\forall j \in \Omega$, taking world GDP as the numeraire at each t.
   (c) Iterate on the following mappings:
      i. Update $P^j_{n,t}$ for $j \in \Omega$ using (10), and obtain $P^E_{n,t}$ from (7).
      ii. Compute trade shares $\pi^j_{mn,t}$ using (12).
      iii. Solve for total expenditure $X^j_{n,t}$ using (13) and (14). Combining (13) and (14) yields

$$X^j_{n,t} = \sum_{j' \in \Omega} \gamma^{M,j'j}_{n,t}\, \gamma^{j'}_{n,t} \sum_{m=1}^{N} \frac{\pi^{j'}_{mn,t}}{(1+\tau^{j'}_{mn,t})(1-s^{j'}_{m,t})}\, X^{j'}_{m,t} \;+\; X^{F,j}_{n,t}, \tag{D.2}$$

      where $X^{F,j}_{n,t} = P^j_{n,t} C^j_{n,t}$ for $j \in \Omega^*_K$ and $X^{F,j}_{n,t} = P^j_{n,t} I^j_{n,t}$ for $j \in \Omega_K$. The term $P^j_{n,t} C^j_{n,t}$ is given by (20), and $I^j_{n,t}$ by (D.1).
      iv. Obtain $Y^j_{n,t}$ from (13).
   (d) Update $\mathbf{w}$ and $\mathbf{r}$: using the trade shares and total expenditures, check the market-clearing conditions (15) and (16); iterate until they are satisfied.
   (e) Move to $t = 2$. Given $\{\varphi^k_{n,1}\}$, update stocks using (18) and (D.1):

$$K^k_{n,2} = \chi_k \left(\varphi^k_{n,1} K^k_{n,1}\right)^{\alpha} (K^k_{n,1})^{1-\alpha} + (1-\delta) K^k_{n,1}.$$

   (f) Repeat steps (a)–(e) for $t = 2, \dots, T$.
4. Plug the resulting paths $K^k_{n,t}$ into the Euler equation to compute the excess demand $Z^k_{n,t}$ for

[10] For equipment productivities, the initial values are given and evolve *endogenously* through learning-by-doing (LBD).

each n, k, t:

$$Z^k_{n,t}\left(\{\varphi^k_{n,t}\}_{t=1}^T\right) = \beta\alpha\left[r^k_{n,t+1} + \frac{(1-\alpha)\,p^k_{n,t+1}I^k_{n,t+1}}{\alpha K^k_{n,t+1}} + \frac{(1-\delta^k)\,p^k_{n,t+1}}{\alpha\chi_k}\left(\frac{I^k_{n,t+1}}{K^k_{n,t+1}}\right)^{1-\alpha}\right] - \frac{u'(C_{n,t})}{u'(C_{n,t+1})}\frac{P_{n,t+1}}{P_{n,t}}\frac{p^k_{n,t}}{\chi_k}\left(\frac{I^k_{n,t}}{K^k_{n,t}}\right)^{1-\alpha}. \tag{D.3}$$

5. Update the investment-rate guess from Step 2 using the excess demand:

$$\varphi^{k,\text{NEW}}_{n,t} \;=\; \varphi^k_{n,t} + \psi\, Z^k_{n,t}\left(\{\varphi^k_{n,t}\}_{t=1}^T\right) \quad \forall\, n, k, t.$$

6. Repeat Steps 2–5 until convergence to a fixed point for $\{\varphi^k_{n,t}\}_{n=1,\ldots,N;\,t=1,\ldots,T}$.